Structure of high-spin nuclear states found from Coulomb excitation

C. Briançon

Center of Nuclear Spectrometry and Mass Spectrometry, Orsay, France

I. N. Mikhaĭlov

Joint Institute for Nuclear Research, Dubna
Fiz. Elem. Chastits At. Yadra **13**, 245–299 (March–April 1982)

The experimental data obtained in recent years on states with angular momenta up to $30\hbar$ in nuclei in the region of the actinides are reviewed. The latest experimental methods employed to study high-spin states in multiple Coulomb excitation experiments are briefly described. Theoretical models which make it possible to analyze the experimental information in terms of alignment of the internal angular momentum along the direction of the rotation axis of the nucleus are described. The rotational properties of aligned nuclear states are discussed.

PACS numbers: 21.10.Re, 27.90. + b, 25.70.Fg, 23.20.Lv

INTRODUCTION

Rotational bands in nuclei were discovered about 25 years ago[1] and were the stimulus for the development of an important direction in the study of nuclear structure. The generalized nuclear model[2] explained many features in the spectra and electromagnetic properties of "rotating," i.e., deformed, nuclei and was convenient for detailed study of quasiparticle and collective degrees of freedom in nuclei. However, even now these problems are as topical as ever. The reason for this is the rapid development of experimental possibilities, which makes it possible to study states with ever larger angular momenta and to obtain more accurate information in the region of intermediate and small angular momenta. Coulomb excitation of nuclei is still an important experimental method of obtaining information about high-spin states of nuclei.[3-6] The use of this important mechanism for generating high-spin states on the basis of heavy-ion accelerators in conjunction with modern techniques for radiation detection is generating a flood of new data on nuclear structure.

For a considerable time, the information on deformed nuclei could be interpreted by assuming that such nuclei have a fairly high rigidity with respect to the excitation of intrinsic degrees of freedom. In other words, the rotation was regarded as slow compared with the motions associated with intrinsic excitations. The mutual influence of rotation and the intrinsic excitation (coupling of the rotation and intrinsic excitations) was either ignored or taken into account by perturbation theory.[7,8] Obviously, such an approach can correspond to reality only when the angular momenta are not too large and the centrifugal and Coriolis forces are insufficiently strong to influence the nuclear structure. An example of the γ spectrum of a good rotator is given in Fig. 1 (taken from Ref. 9), which shows the spectrum of ^{233}U excited by the Coulomg field of a heavy ion (^{84}Kr, $E_{lab}=460$ MeV). The set of approximately equidistant lines in Fig. 1 corresponds to collective E2 transitions to the ground-state band ($K=7/2$) of the nucleus ^{233}U. In each transition, the angular momentum I of the nuclear state decreases by two Planck units. In view of the obvious correspondence with classical mechanics, the expression

$$\omega^{\text{rot}}(I)=(E(I+1)-E(I-1))/2\approx dE(I)/dI, \tag{1}$$

which contains the energy $E(I)$ of the states, is called the angular frequency of the rotation corresponding to the angular momentum I, and the ratio

$$(I+1/2)/\omega^{\text{rot}}=J \tag{2}$$

is called the effective moment of inertia of the state. Equidistant spacing of the lines in the γ spectra corresponds to a linear dependence of ω^{rot} on I and a constant moment of inertia J for all states of the corresponding part of the spectrum.

More careful examination of Fig. 1 reveals that J increases in the ground-state band of ^{233}U with increasing angular momentum, indicating a coupling between the rotation and the intrinsic structure of the nucleus. The possible existence of clear manifestations of such coupling was noted[10,11] in 1960, when a weakening of the pair correlations by Coriolis forces was predicted. Approximately ten years later, clear manifestations of coupling of rotation to the intrinsic excitations were observed experimentally,[12] it being found that in a number of nuclei the dependence of the moment of inertia (2) on the angular frequency of the rotation ceases to be monotonic. The γ spectrum of ^{158}Er with anomalous dependence of the moment of inertia on the angular frequency is shown in Fig. 2.[13] It is now well known that the first anomaly of the moment of inertia is not related to a phase transition from a state with pairing to one without pairing correlations,[14,15] though it was found as the result of a search for such a phase transition. The anomaly was found to be due to a change in the configuration of the quasiparticles in the lowest states of the nuclei with increasing I under conditions when the pairing is not yet significantly suppressed by the Coriolis forces.

The discovery of the anomalous dependence indicated that rotation can strongly influence the structure of a nucleus, and it stimulated systematic investigations in the high-spin region. The results of these studies at high angular momenta indicate that the structure of nu-

 0090-4759/82/020101-23$04.40

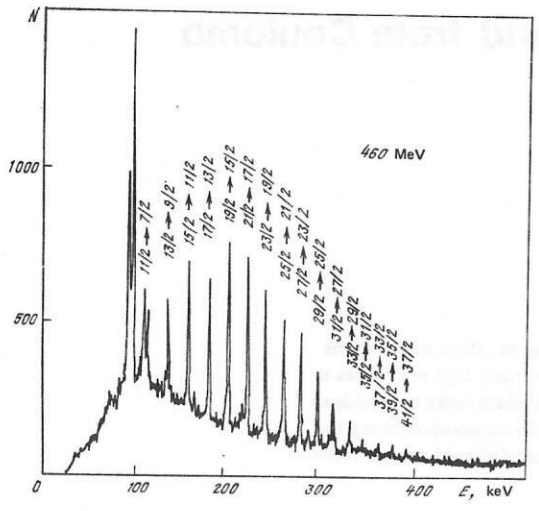

FIG. 1. Coulomb excitation of ^{233}U by ^{84}Kr nuclei at energy $E = 460$ MeV in the laboratory system. The γ photons were detected in coincidence with the scattered particle.[9]

clei does indeed undergo significant modifications with increasing angular momentum. The present review is devoted to the best studied changes of the structure in the high-spin region. The central theme of the review is, in fact, the effects generated by alignment of the angular momenta, associated with the intrinsic degrees of freedom of the nucleus, along the direction of the total (collective) angular momentum. The alignment of the angular momenta leads to changes in the nucleon distribution function in the momentum or angular-momentum space. The symmetry type of the wave function of the nucleus is changed, and also the selection rules for the electromagnetic transitions. In the review, we attempt to trace the characteristic changes associated with alignment in the selection rules for the electromagnetic transitions.

Limitations of space have forced us to omit a consideration of the data on the change in nuclear shape due

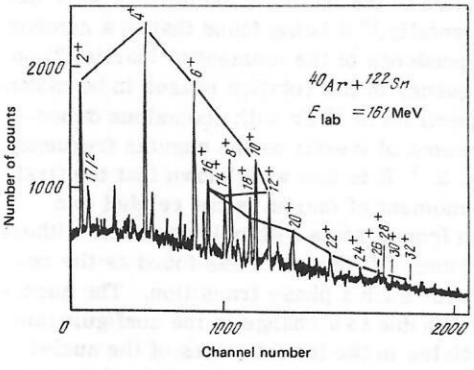

FIG. 2. Spectrum of the γ radiation of the products of the reaction ^{122}Sn(^{40}Ar, xn)$^{162-x}$Er at $E(^{40}\text{Ar}) = 161$ MeV obtained using a Ge–Li detector.[13] The figure shows the lines of the known $I \to I-2$ transitions along the yrast line of ^{158}Er (up to $I = 32$). One can clearly see an anomaly in the dependence of the transition energy on I in the region $12 \leq I \leq 16$; the following intersection of the bands corresponds to the breakdown in the regular ordering of the lines around $I = 28$.

to rotation. We believe that this subject should be treated in a separate paper.

The review is arranged as follows.

In Sec. 1, we give the elements of the theory used subsequently to analyze the structure of aligned states.

Section 2 contains material on the alignment of the angular momentum of quasiparticle states in odd nuclei.

In Sec. 3, we study the alignment of the collective angular momentum in negative-parity states. We here give a simple phenomenological model of octupole bands distorted by Coriolis forces. In particular, this model makes it possible to give a simple geometrical interpretation to the selection rules for electric dipole transitions from the states of an aligned octupole band to a state of the ground band.

1. SYMMETRY OF THE WAVE FUNCTIONS OF HIGH-SPIN STATES. ASYMPTOTIC EXPRESSION FOR THE MATRIX ELEMENTS

To study the structure of high-spin states, it is helpful to modify somewhat the usual formulation of the collective model with a view to having:

1) the possibility of an adequate choice of intrinsic states of quasiparticle and collective type;

2) expressions for the matrix elements of the physical observables and, on this basis, selection rules for the various nuclear transitions.

The difficulty encountered in achieving these aims is that the condition of adiabatically slow rotation, $\omega^{\text{rot}} \ll \omega^{\text{intr}}$, where ω^{intr} is the frequency of the excitations of nonrotational type, ceases to hold when $I \gg 1$.

An approximate expression for calculating the matrix elements that can be used under a very wide range of conditions when $I \gg 1$ can be formulated using some weak assumptions.[16] The main assumption, which leads to an asymptotic expression for the matrix elements, is as follows. Suppose that in the nuclear states situated in the neighborhood of the yrast line the angular momentum has a fairly well-defined and constant (in time) orientation in a suitably chosen intrinsic coordinate system. Such an assumption is based on the experience gained from studying the rotation of macroscopic objects. "Secular equilibrium" of a rotating body is attained when the angular momentum is directed along the longest axis of the inertia tensor of the rotating body. Such an assumption is not a novelty in nuclear physics, and it is used to analyze the shape of rotating nuclei; the spectrum of a triaxial rigid rotator was analyzed on this basis by Bohr and Mottelson.[17] The assumption is quasiclassical in nature, since the noncommutativity of the angular-momentum operators leads to uncertainty relations for the probabilities of all three of its projections in any coordinate system. However, for $I \gg 1$ such uncertainty relations should not be important.

To formalize the assumption, we introduce angular variables Ω, which fix the orientation of the nucleus in space, and intrinsic variables ξ, these forming together

with Ω a complete set of variables determining the configuration of the nucleus. We do not require the explicit form of the expressions that relate Ω and ξ to the coordinates of the nucleons in the nucleus; to have a clear picture, we can assume that these variables are defined as in the papers of the Kiev group[18] (and then the orientation of the nucleus in space is specified by the directions of the principal axes of its inertia tensor). We represent the wave function of the nucleus in the form of the expansion

$$|\alpha IM\rangle = \left(\frac{2I+1}{8\pi^2}\right)^{1/2} \sum_{\tau=0}^{2I} c_\tau^{\alpha I} D^I_{MI-\tau}(\Omega)\, \Phi_{\alpha I\tau}(\xi), \tag{3}$$

where the normalized functions $\Phi_{\alpha I\tau}$ depend only on the intrinsic variables, $c_\tau^{\alpha I}$ are weight coefficients ($\sum_\tau |c_\tau|^2 = 1$), and, finally, $D^I_{MM'}(\Omega)$ are generalized spherical functions.[19] As the quantization axis in the intrinsic coordinate system we choose the axis along which the angular momentum is predominantly aligned in the states of the yrast line. Then the following conditions must be satisfied:

$c_\tau^{\alpha I}$ is essentially nonzero if $\tau \ll I$.

We now consider the multipole operator $\hat{\mathcal{M}}(\lambda, \mu)$, where we understand by λ and μ indices that determine the transformation properties of the operator with respect to the rotation group in the laboratory coordinate system. We shall assume that the multipole order of the operator is not large, so that the condition $\lambda \ll I$ is satisfied. Expressing the coordinates of the nucleons in terms of the variables Ω and ξ, we arrive at the usual expression for the operators[17]:

$$\hat{\mathcal{M}}(\lambda, \mu) = \sum_{\tau=-\lambda}^{\lambda} D^\lambda_{\mu\tau}(\Omega)\, \hat{\mathcal{M}}'(\lambda, \tau; \xi), \tag{4}$$

which contain the operators of the intrinsic multipole moments $\hat{\mathcal{M}}'(\lambda\tau; \xi)$. The expression (4) corresponds to an operator of "electric type," which does not depend on the nucleon momenta. Operators of magnetic type can be considered similarly.

Using the expressions (3) and (4), we write down the expression for the matrix element $\langle \alpha_2 I_2 M_2 | \hat{\mathcal{M}}(\lambda\mu) | \alpha_1 I_1 M_1 \rangle$ and integrate over the angular variables Ω, obtaining

$$\begin{aligned}&\langle \alpha_2 I_2 M_2 | \hat{\mathcal{M}}(\lambda\mu = M_2 - M_1) | \alpha_1 I_1 M_1 \rangle \\ &= \sum_{\tau_1\tau_2\tau_3} c^{\alpha_2 I_2 *}_{\tau_2} c^{\alpha_1 I_1}_{\tau_1} (\lambda\mu I_1 M_1 | I_2 M_2)\, (\lambda\tau_3 I_1 I_1 - \tau_1 | I_2 - \tau_2) \\ &\quad \times \langle \Phi_{\alpha_2 I_2 \tau_2}(\xi) | \hat{\mathcal{M}}'(\lambda\tau_3) | \Phi_{\alpha_1 I_1 \tau_1}(\xi) \rangle.\end{aligned} \tag{5}$$

The Clebsch–Gordan coefficients $(\lambda\mu I - \tau M - \mu | IM)$ in Eq. (5) can be replaced by the asymptotic expressions for them which hold when $\lambda \ll I$ (Ref. 19)[1)]:

$$(\lambda\mu\ I - \tau\ M - \mu | IM) \approx (-1)^{\lambda-\tau} D^\lambda_{\mu\tau}(0,\ \arccos(M/I),\ 0). \tag{6}$$

Using the condition that the coefficients $c_\tau^{\alpha I}$ are small at large τ, we obtain

$$\begin{aligned}&\langle \alpha_2 I_2 M_2 | \hat{\mathcal{M}}(\lambda M_2 - M_1) | \alpha_1 I_1 M_1 \rangle \\ &\approx D^\lambda_{\mu I_2 - I_1}(0,\ \arccos(M/I),\ 0)\, \langle \alpha_2 I_2 | \hat{\mathcal{M}}'(\lambda,\ \tau = I_2 - I_1) | \alpha_1 I_1 \rangle,\end{aligned} \tag{7}$$

where we have introduced the following notation for an intrinsic matrix element:

$$\begin{aligned}&\langle \alpha_2 I_2 | \hat{\mathcal{M}}'(\lambda\tau) | \alpha_1 I_1 \rangle = \sum_{\tau'} c^{\alpha_2 I_2 *}_{\tau'} c^{\alpha_1 I_1}_{\tau'} \\ &\times \langle \Phi_{\alpha_2 I_2 \tau'}(\xi) | \hat{\mathcal{M}}'(\lambda\tau;\ \xi) | \Phi_{\alpha_1 I_1 \tau'}(\xi) \rangle.\end{aligned} \tag{8}$$

It is helpful to express (7) and (8) in a somewhat different form, for which we introduce new notation for the state vector:

$$|\alpha I\rangle = \begin{pmatrix} \vdots \\ c_\tau^{\alpha I} \\ c_{\tau+1}^{\alpha I} \\ \vdots \end{pmatrix} \tag{9}$$

and for the operator of the intrinsic multipole moment:

$$\mathfrak{M}'(\lambda\tau) = D[\ \ldots \langle \Phi_{\alpha_2 I_2 \tau'}(\xi) | \hat{\mathcal{M}}'(\lambda\tau;\ \xi) | \Phi_{\alpha_1 I_1 \tau'}(\xi) \rangle \ \ldots], \tag{10}$$

where $D[\ ]$ is a diagonal matrix. Equation (7) takes the form

$$\begin{aligned}&\langle \alpha_2 I_2 M_2 | \hat{\mathcal{M}}(\lambda,\ \mu = M_2 - M_1) | \alpha_1 I_1 M_1 \rangle \\ &\approx D^\lambda_{\mu,\ I_2 - I_1}(0,\ \arccos(M/I),\ 0)\, \langle \alpha_2 I_2 | \mathfrak{M}'(\lambda,\ \tau = I_2 - I_1) | \alpha_1 I_1 \rangle.\end{aligned} \tag{11}$$

In such a form, the expression for the matrix elements can also be used for operators of more general form than in (4). However, Eq. (10) ceases to hold if the operators $\mathcal{M}'(\lambda, \tau)$ depend on the angular momenta. In particular, for the operators $J'_0, J'_{\pm 1}$ of the angular-momentum projections onto the intrinsic axes, which we define as in the monograph of Ref. 19 (p. 66), we can readily obtain the approximate expressions

$$\begin{aligned}&J'_0 = -(I - b^+ b); \\ &J'_{+1} = -J'^+_{-1} = \sqrt{I}\, b = \sqrt{I} \begin{pmatrix} \ddots & & \\ & 0 & \sqrt{\tau'} \\ & 0 & 0 \\ & & \ddots \end{pmatrix},\end{aligned} \tag{12}$$

which are known, for example, as the high-spin limit of the boson representation of angular-momentum operators.[20]

The expression (11) is the expression we require for the matrix element valid when $I \gg 1$. To use it, it is not necessary to know at all the series expansion (4) of the wave function, and one can take any convenient representation for the state vector (9). In Sec. 3, we use this expression to analyze electric transitions from "aligned" states.

To analyze the symmetry properties of nuclear states for $I \gg 1$, additional hypotheses are needed. If the precise dependence of the functions $\Phi_{\alpha I\tau}(\xi)$ on τ is not exceptionally important, we can introduce as basis functions in the intrinsic space the eigenfunctions of the operator[21]

$$\hat{H}^I_\xi = \int d\Omega u^*_{IM}(\Omega)\, \hat{H} u_{IM}(\Omega), \tag{13}$$

where $\hat{H}$ is the total Hamiltonian of the nucleus defined in the complete space of the variables, and

$$u_{IM}(\Omega) = ((2I+1)/8\pi^2)^{1/2} \sum_{M'} D^I_{MM'}(\Omega)\, D^I_{M'I}(\Omega_0) \tag{14}$$

[1)] Translator's Note. The Russian notation for the trigonometric, inverse trigonometric, hyperbolic trigonometric functions, etc., is retained here and throughout the article in the displayed equations.

is the so-called coherent function of a quantum rotator.[22] The coherent functions have the property that they minimize the uncertainty $\sum_{i=1}^{3}\langle(\hat{J}_i' - \langle\hat{J}_i'\rangle)^2\rangle$ in the orientation of the angular momentum. The coherent functions have exact values of the quantum numbers I and M of the angular momentum and are completely determined by specification of the angular parameters $\Omega_0 \equiv(\Phi, \theta, 0)$ $(0 \leqslant \theta \leqslant \pi, 0 \leqslant \Phi \leqslant 2\pi)$. The same parameters Φ and θ characterize the orientation of the angular momentum in the intrinsic coordinate system:

$$\Big(\sum_{i=1}^{3} n_i \hat{J}_i'\Big)\, u_{IM}(\Omega) = I u_{IM}(\Omega), \tag{15}$$

if

$$n_1 = \cos\Phi \sin\theta, \quad n_2 = \sin\Phi\sin\theta, \quad n_3 = \cos\theta. \tag{16}$$

For the nonrelativistic Hamiltonian

$$\hat{H} = \sum_{i=1}^{3} (A_i(\xi)\hat{J}_i'^2 + \hat{B}_i(\xi)\hat{J}_i) + \hat{\mathscr{H}}(\xi) \tag{17}$$

the "intrinsic" Hamiltonian defined by (13) takes the form

$$\hat{H}_\xi^I = \sum_{i=1}^{3} [(I(I-1/2)n_i + I/2)A_i(\xi) + I n_i \hat{B}_i(\xi)] + \hat{\mathscr{H}}(\xi). \tag{18}$$

The analogy drawn earlier with classical mechanics gives grounds for assuming that the angular momentum in the states of the yrast line is directed along one of the principal axes of the inertia tensor, which in such a case can be taken as the first axis. Then $n_i = (1, 0, 0)$, and

$$\hat{H}_\xi^I = I^2 A_1(\xi) + I\hat{B}_1(\xi) + \hat{\mathscr{H}}(\xi). \tag{19}$$

This last operator has the same symmetry properties as the Hamiltonian of the nucleus in the cranking model, namely, it is invariant with respect to a transformation corresponding to rotation of the coordinate system through angle π about the rotation axis, i.e., about axis 1:

$$\hat{R}_1^{-1}(\pi)\,\hat{H}_\xi^I R_1(\pi) = \hat{H}_\xi^I. \tag{20}$$

Then the eigenfunctions $\Phi_{\alpha I}(\xi)$ of the operator $\hat{H}_\xi^I$,

$$\hat{H}_\xi^I \Phi_{\alpha I}(\xi) = e_{\alpha I}\Phi_{\alpha I}(\xi), \tag{21}$$

are such that they can be endowed with a quantum number σ (signature) such that

$$\hat{R}_1(\pi)\,\Phi_{\alpha I}(\xi) = \sigma_\alpha \Phi_{\alpha I}(\xi) \quad (|\sigma_\alpha| = 1). \tag{22}$$

The specification of the nucleon coordinates does not uniquely determine the orientation of the inertia tensor of a nucleus.[18] In particular, when the inertia tensor is rotated through π about any of its axes, the position of the nucleons remains unchanged. The nuclear wave function, which is a single-valued function of the nucleon coordinates, is not changed by such a transformation. Writing the wave function of the nucleus in the form

$$\Psi_{\alpha IM} = u_{IM}(\Omega)\,\Phi_{\alpha I}(\xi) \tag{23}$$

and using the transformation properties of the coherent functions,

$$\hat{R}_1(\pi)\,u_{IM}(\Omega) = (-1)^I u_{IM}(\Omega), \tag{24}$$

we arrive at the important selection rule

$$(-1)^I \sigma_\alpha = 1. \tag{25}$$

The selection rule (25) means that intrinsic states with given signature can be encountered only for I values which satisfy this equation. If $\Phi_{\alpha I}(\xi)$ varies slowly with I, the nuclear states then form series that include as well as a state with a certain value of the spin I states with

$$I' = I \pm 2, \quad I \pm 4 \tag{26}$$

etc. Such series of states (bands) can be clearly seen in the spectra of odd nuclei (Fig. 3).[23]

The construction of the collective model given in this section can be continued by determining a complete basis of states of the type (23), with respect to which the nuclear wave function can be expanded.[21] In this way, one can study the mixing of states with different intrinsic functions $\Phi_{\alpha I}(\xi)$. The treatment given in Ref. 21 shows that the signature is an asymptotic quantum number describing the states when

$$I \gg 1, \tag{27}$$

provided the intrinsic functions $\Phi_{\alpha I}(\xi)$ change sufficiently slowly with increasing angular momentum. Mixing of states with different signature can evidently be expected only under exceptional conditions, an example of which is considered in Ref. 15.

2. ALIGNMENT OF THE ANGULAR MOMENTUM IN THE CONFIGURATIONS OF THE GROUND STATES OF ODD AND EVEN-EVEN NUCLEI

Experimental methods of studying high-spin states

During the last few years, many new experimental results have been obtained for well-deformed nuclei. This was made possible by the develop-

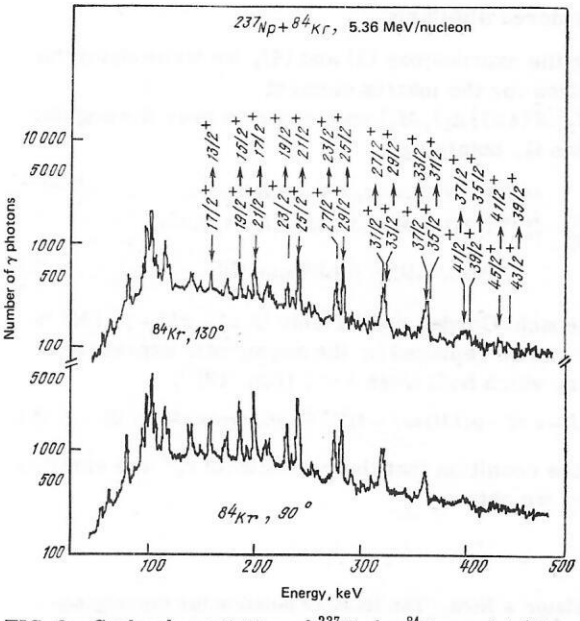

FIG. 3. Coulomb excitation of ^{237}Np by ^{84}Kr nuclei (E_{lab} = 5.36 MeV/nucleon); the spectrum of γ photons in coincidence with a particle scattered through 130 or 90°.[23]

ment of a very subtle experimental method, and also by the possibility of using beams of heavy ions.

A large angular momentum (up to $70\hbar$ for the nuclei of rare-earth elements) can be communicated to a nucleus in a reaction induced by a heavy ion, for example, a (HI, xn) reaction. However, the states produced directly after fusion of heavy ions are situated far from the yrast line, and they decay through a huge number of different channels. Therefore, the γ photons emitted during the decay of high-spin states obtained in heavy-ion reactions form a quasicontinuous spectrum consisting of a large number of overlapping discrete lines. Individual lines in such spectra can be observed only when

$$I \leqslant 35\hbar. \qquad (28)$$

The γ spectra from heavy-ion reaction products have been successfully studied using various γ filters, for example, a filter with selection of the photon multiplicity[13] or the total energy of the photons.[24]

In multiple Coulomb excitation, an angular momentum of up to about $30\hbar$ can be communicated to nuclei by using very heavy ions such as ^{208}Pb. At the present time, multiple Coulomb excitation is the most promising method of producing high-spin states, especially in the region of the actinides, on which we shall concentrate; under standard conditions of a heavy-ion reaction, the fission channel is dominant for these nuclei.

Multiple Coulomb excitation and (HI, xn) reactions are the most convenient sources of information about high-spin states of nuclei. These two processes complement each other. In (HI, xn) reactions, states on or near the yrast line are populated after the emission of a few particles and γ photons; the method can be used basically to study neutron-deficient nuclei. In the case of multiple Coulomb interaction, there is excitation of not only the states of the yrast line but also many other states strongly coupled by electromagnetic interactions to states of the ground rotational band. Of course, this method can be used only for stable or very long-lived nuclei, i.e., for nuclei with a large number of neutrons.

In experiments with Coulomb excitation of a heavy ion, it is very difficult to observe γ photons with good energy resolution, since the photons emitted by a moving scattered nucleus ($v/c \approx 0.1$) have an appreciable Doppler shift, and their spectrum is smeared because of the distribution of the nuclei with respect to the recoil velocity and the scattering angle, and also because of the finite size of the γ detector. There are two possibilities for overcoming these difficulties:

1) the use of thick targets with a backing in which the recoil nuclei are stopped in a few picoseconds;

2) the use of thin targets and the identification of both colliding particles in detectors sensitive to the position of the detected particles in space.

Experiments with thick targets. In experiments with heavy ions such as krypton, in which states with angular momenta up to $20\hbar$ can be populated in multiple Coulomb excitation, the time required to stop the recoil nuclei is shorter than or comparable with the lifetime of the last generated states. This makes it possible to perform direct measurements of the γ photons and make coincidence measurements with very good resolution by means of the experimental arrangement (Fig. 4) employed at Orsay in systematic investigations into the structure of nuclei in the region of the actinides.[9,25-30]

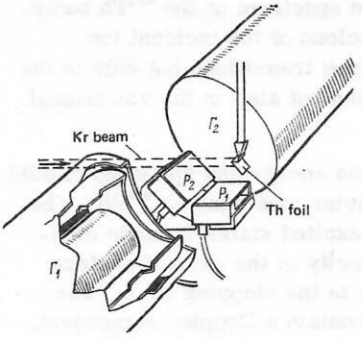

FIG. 4. Arrangement for studying Coulomb excitation of actinides with ^{84}Kr beam in γ-photon coincidence experiments. A thick target is inclined at 45° to the beam. Each of the two particle detectors P_1 and P_2 (boron implanted in silicon) has an effective surface measuring 25×22 mm and covers the scattering angles from 70 to 150°. The two γ-ray Ge–Li detectors Γ_1 and Γ_2 are situated at right angles on either side of the beam of incident ions.[5,25]

The arrangement was used in conjunction with the heavy-ion accelerator ALICE, and it made it possible to observe γ photons in coincidence with scattered ions of the ^{84}Kr beam detected in two silicon detectors with implanted boron nuclei, and also $\gamma\gamma$ coincidences in two Ge–Li detectors placed at ±90° relative to the beam axis and perpendicular to the plane of the reaction fixed by the particle detector. The detectors detect particles in the range of angles from 70 to 150° and have mean angular coordinates at 90 and 130°, respectively. The dependence of the γ intensity on the scattering angle of the particles contains valuable information about the position of the γ transition in the nuclear cascade. In addition, the high statistics and good resolution of the $\gamma\gamma$ coincidences are important properties of the facility for unique determination of states with spins up to $20\hbar$ belonging to the ground and excited bands.

An example of the spectrum for a γ photon in coincidence with a scattered particle is given in Fig. 5,

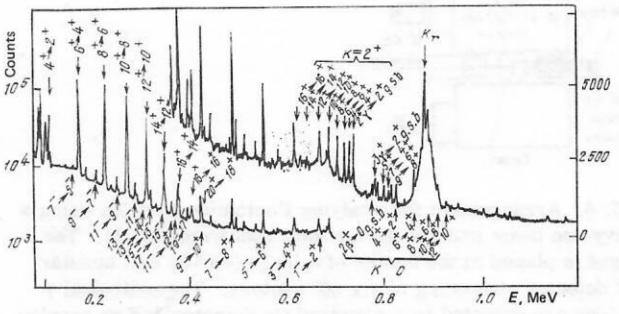

FIG. 5. Coulomb excitation of ^{232}Th by ^{84}Kr ions at $E = 5.35$ MeV/nucleon. The spectrum of γ photons in coincidence with a particle scattered backward.[27]

which shows the excitation spectrum of the ^{232}Th nucleus at energy 5.35 MeV/nucleon of the incident ion (^{84}Kr).[27] Here, one observes transitions not only in the ground-state rotational band but also in the vibrational octupole, β, and γ bands.

States with high excitation energy and spins (up to $30\hbar$) can be observed using heavier ions such as ^{208}Pb. The identification of the most excited states is made difficult by the high recoil velocity of the excited nucleus and the resulting increase in the stopping time. The lines of the γ transitions contain a Doppler component, from which one can determine the lifetimes of the corresponding states if the measurements are organized in such a way that one can control the "feeding" of the investigated states by γ transitions from the more highly excited part of the spectrum. The method which uses a filter with respect to the total energy of the γ photons (a total spectrometer) is illustrated in Fig. 6. This instrument was used with the UNILAC at the GSI in a number of experiments with nuclei in the rare-earth and actinide regions.[23,30-34]

In the experiment, there was an annular NaI detector measuring 40 × 30 cm divided radially into six 60° segments. The target was placed at the center of the crystal, which absorbed the main fraction of the γ photons, and the individual γ photons were detected by a standard Ge detector and an annular Ge detector, these two detectors being placed at 0 and 180° with respect to the beam. Ensuring coincidences with a pulse of the total spectrometer of the desired intensity, one can choose the start of the γ decay observed by both Ge detectors. In this way, one can realize a control on the "feeding" of the investigated state. More precisely, the arrangement makes it possible to select events associated with high spins by ensuring a high multiplicity of γ photons with the aim of ensuring that only the last populated levels decay, emitting γ photons whose lines are broadened by the Doppler shift. An example of a γ spectrum with selection for study of high-spin events is shown in Fig. 7. In this experiment, the excitation spectrum of ^{232}Th was studied, the thorium nuclei being used as beam ions stopped in a ^{208}Pb target.[32] Such an experiment is preferable because the stopping time is shortened when the roles of the projectile and target are interchanged.

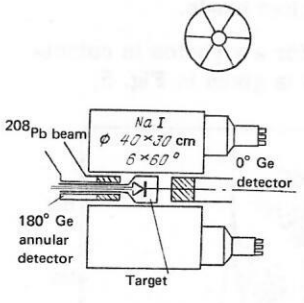

FIG. 6. Arrangement for studying Coulomb excitation using a heavy-ion beam and six-sector total spectrometer (1). The target is placed at the center of a large (40×30 cm) annular NaI detector consisting of six 60° sectors. The individual γ photons are detected by a standard Ge detector and an annular Ge detector placed at 0° and 180°, respectively, relative to the beam. The equipment and experiment are described in detail in Ref. 23.

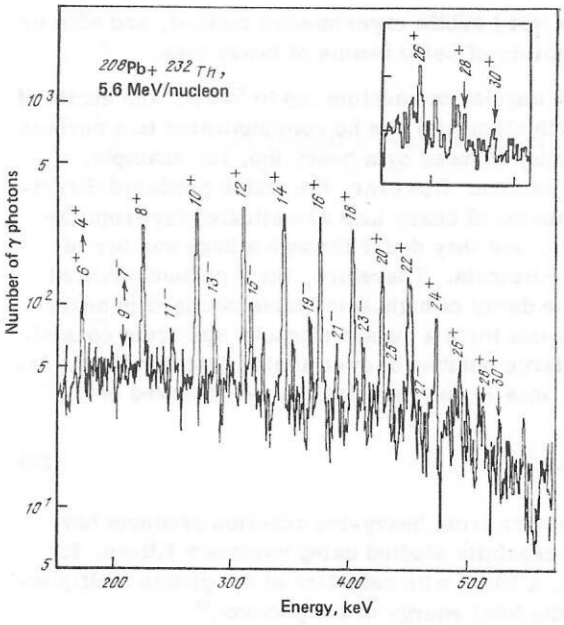

FIG. 7. Coulomb excitation of nuclei of a ^{232}Th beam observed in the backward Ge detector. The chosen events correspond to a high total energy and the requirement that five or six sectors of the spectrometer respond.[32]

Experiments with thin targets. In multiple Coulomb excitation experiments in thin targets without backing (≤ 1 mg/cm^2), the recoil nuclei are emitted into vacuum with such high velocites that measurement of the spectra using the observation of individual γ photons is impossible. A method for correcting the Doppler shift of the photons was developed in Refs. 6, 31, and 35. The experimental arrangement is shown in Fig. 8. The γ photons are observed in coincidence with the Coulomb-excited recoil nuclei, which are detected in a shower detector that is sensitive to the particle position and covers solid angle

$$15° \leqslant \theta \leqslant 60°; \tag{29}$$

$$-25° \leqslant \varphi \leqslant 25° \tag{30}$$

(the angle φ determines the position in the plane perpendicular to the figure). The cathode of the detector is divided into narrow strips, which correspond to curves with the same scattering angle and are joined in such a

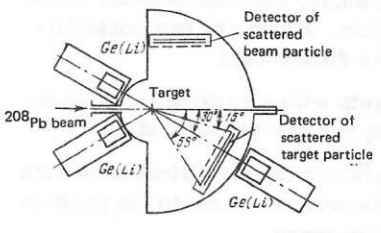

FIG. 8. Arrangement for studying multiple Coulomb excitation in experiments with thin targets.[35] The position of the detector of the beam particles and the Ge(Li) detectors is fixed, while the position of the detector of the target particles is determined by the ratio of the target and beam particle masses.

way that a delay line is formed, this yielding information about the scattering angle. On the basis of this information, it is possible to correct for the Doppler shift. To distinguish the target recoil nucleus from the scattered beam particle, a further detector is used in a position that depends on the combination of the nuclei participating in the reaction. Thus, using the kinematic correlations between the two particles detected in coincidence, and also information on the time of flight, which is different for the beam and target particles, it is possible to distinguish the two types of event. Figure 9 shows different stages in the numerical analysis of the experimental data, beginning with the observation of the spectra of the individual γ photons (a) and then, below, the spectra of γ photons in coincidence with a particle detected in the particle detector (b); then comes the same spectrum corrected for the Doppler shift (c), and, finally, the corrected γ spectrum (d) corresponding to only Dy recoil nuclei.[6]

This method was used to study deformed nuclei of rare-earth elements[36] and nuclei in the region of the actinides (Refs. 31, 33, 34, 37, and 38). Examples of spectra obtained in this manner are shown in Figs. 10 and 11. The Doppler-corrected spectrum obtained in the case of Coulomb excitation of ^{248}Cm by ^{208}Pb ions[38] is shown in Fig. 10. Spectra of the odd nuclei ^{235}U and ^{237}Np are shown in Fig. 11.[34] In the upper part of the figure, we show the ^{237}Np spectrum with Doppler-shift correction, in the middle the analogous ^{235}U spectrum, and at the bottom, for comparison, the ^{235}U spectrum obtained in an experiment with a thick target using a total spectrometer with the best resolution.

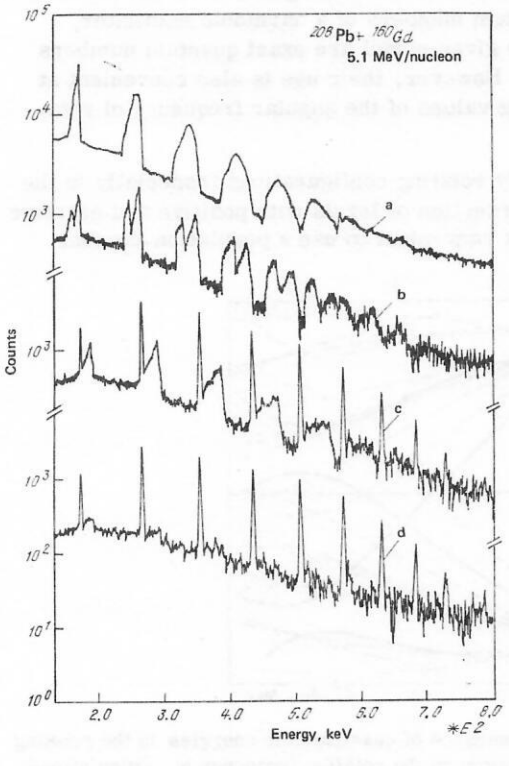

FIG. 9. Example of analysis of experimental data obtained in an experiment with thin targets in the case of Coulomb excitation of ^{164}Dy by ^{208}Pb ions at E= 4.7 MeV/nucleon.[6]

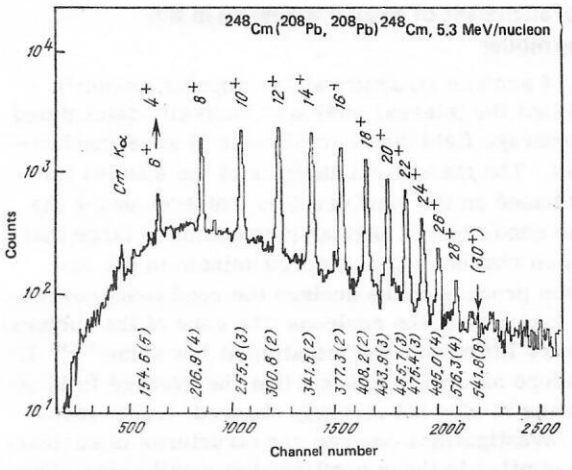

FIG. 10. Spectrum with correction for Doppler shift corresponding to γ emission of ^{248}Cm after scattering with small impact parameter.[38]

Such experimental results, found by means of these two complementary methods, made it possible to obtain very complete information about the yrast configurations and the bands of excited states in nuclei in the actinide region. In the following parts of this paper, we shall review the theoretical methods used to study nuclear structure on the basis of these results.

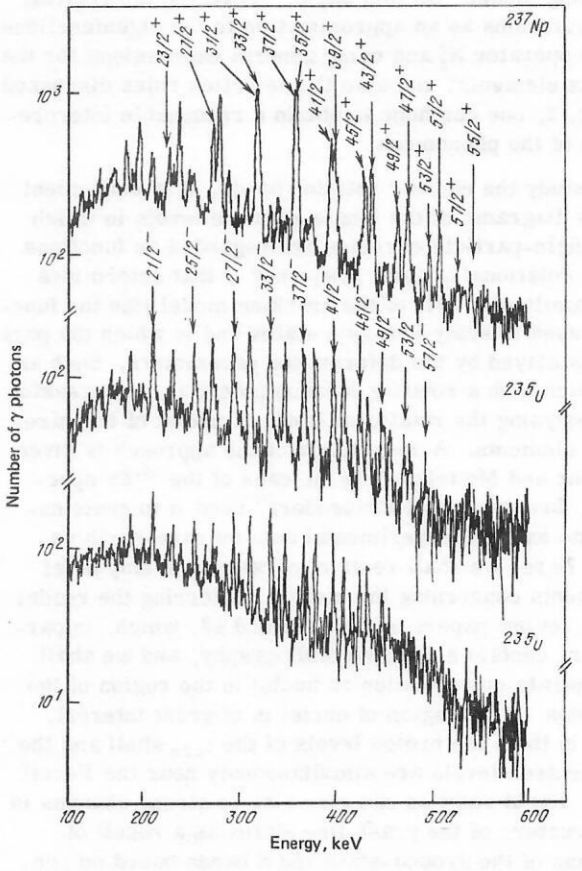

FIG. 11. The γ radiation resulting from Coulomb excitation of ^{235}U and ^{237}Np.[34]

Study of alignment of angular momenta in the cranking model

Study of nuclear structure at low angular momenta showed that the internal motion is basically determined by the average field (and correlations of superconducting type). The theoretical analysis of the spectra for $I \gg I$ is based on the consideration that even under the extreme conditions of angular momentum so large that the fission channel begins to predominate in the de-excitation process of the nucleus the conditions governing the majority of the nucleons (the core of the nucleus) differ very little from the situation at low spins.[15,39] It is therefore natural to assume that the average field of the nucleus is also not strongly changed, and in theoretical investigations one can use structures of nuclear models similar to those confirmed at small spins. One such model is the cranking model, in which it is assumed that the collective rotational angular momentum distinguished a certain direction in space, with respect to which the average field of the nucleus rotates with an angular frequency that is constant in time. Physically, such an assumption is close to the assumptions formulated in Sec. 1. On the basis of them, we introduced the intrinsic Hamiltonian $\hat{H}_\xi^I$ of a rotating nucleus. We note that the symmetry type of $\hat{H}_\xi$ is the same as for the energy operator in a rotating coordinate system,

$$\hat{H}' = \hat{H} - \omega \hat{J}_x, \tag{31}$$

which determines the rotating configurations in the cranking model. On this basis, regarding the rotating configurations as an approximation to the eigenfunctions of the operator $\hat{H}_\xi^I$ and using general expressions for the matrix elements, and also the selection rules discussed in Sec. 2, one can hope to obtain a reasonable interpretation of the phenomena.

To study the nuclear rotation bands, it is convenient to use diagrams of the single-particle levels in which the single-particle energies are regarded as functions of the rotational angular frequency ω that determines the Hamiltonian (31) of the cranking model like the functions used to study low-spin states and in which the part of ω is played by the deformation parameters. Such an approach with a rotating Nilsson potential is successful for analyzing the rotational bands of nuclei of the rare-earth elements. A description of the approach is given by Bohr and Mottelson[40] in the case of the ^{164}Er spectrum; Bengtsson and Frauendorf[41] used it to systematize the existing experimental data on rare-earth nuclei. Here, we shall restrict ourselves to only brief comments concerning the method, referring the reader to the review papers of Refs. 42 and 43, which, in particular, contain a detailed bibliography, and we shall concentrate our attention on nuclei in the region of the actinides. This region of nuclei is of great interest, since in them the proton levels of the $i_{13/2}$ shell and the $j_{15/2}$ neutron levels are simultaneously near the Fermi limit. Rapid rotation can give rise to strong changes in the structure of the yrast-line states as a result of crossing of the ground-state and S bands based on configurations in which the nucleons occupy levels with large j and with internal angular momentum aligned along the collective angular momentum of rotation of the core.

Quasiparticle configurations of a rotating nucleus. The Hamiltonian of a rotating nucleus is given by (31), in which $\hat{H}$ is the Hamiltonian that includes the average field and the pairing correlations, taken into account in the framework of the u–v transformation method, and the angular frequency ω of the rotation is related to the angular momentum I of a state of the rotational band by the canonical relation (1). The Hamiltonian $\hat{H}$ contains the deformation parameters of the field and the chemical potential which ensures description of a system with the desired number of nucleons. The eigenfunctions of the Hamiltonian (31) determine the configurations of the independent quasiparticles, and the eigenvalues determine the excitation energies of the quasiparticle states calculated as functions of ω. Since $\hat{H}'$ is invariant with respect to reflection and rotation through 180° about the x axis, the single-particle states have the parity π and the signature (see Sec. 1) as quantum numbers. The selection rule of states of a definite signature with respect to the angular momentum [Eq. (25)] imposes a restriction on the angular momenta of the states of a band. the signature quantum number α given in Ref. 40 differs in sign from the number σ introduced earlier, and $I_\alpha = \alpha \pmod 2$.

The diagram of the quasiparticle energies of a rotating nucleus as a function of ω is given in Fig. 12. The diagram corresponds to the parameters of the Hamiltonian $\hat{H}$ that describes the nucleus ^{160}Yb.[44] Similar diagrams for actinide nuclei[45] are shown in Fig. 13 (proton system, $Z \approx 91$) and Fig. 14 (neutron system, $N \approx 143$). The levels in the diagrams are also denoted by the quantum numbers of a harmonic oscillator, which in the given model are exact quantum numbers when $\omega = 0$. However, their use is also convenient at nonvanishing values of the angular frequency of rotation.

To classify rotating configurations (especially in the case of intersection of levels with positive and negative energy) it is convenient to use a population-number

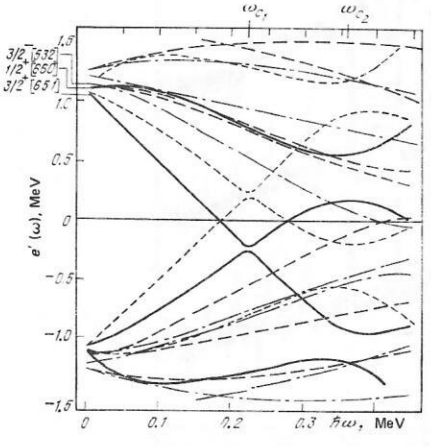

FIG. 12. Dependence of quasiparticle energies in the rotating coordinate system on the rotation frequency ω. Calculations are made in the framework of the cranking model[44] and for the following values of the parameters: $\varepsilon_2 = 0.2$, $\varepsilon_4 = -0.02$, $\Delta = 1.06$ MeV, $\lambda = 6.38\hbar\omega_0$, $N = 90$.

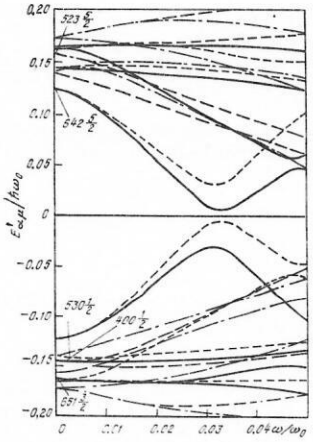

FIG. 13. The same as in Fig. 12 for the proton levels for Z = 91 (Ref. 45); $\lambda = 6.32\hbar\omega_0$, $\varepsilon_2 = 0.24$, $\varepsilon_4 = -0.04$, $\Delta = 0.12\hbar\omega_0$.

representation whose formalism differs somewhat from that usually employed to classify fermion levels. To each level with energy $E'_{\alpha\mu}$ in the diagrams in Figs. 13 and 14 there corresponds a conjugate level $-E'_{\alpha\mu}$, so that the lower part of the diagrams is obtained by reflection of the upper part with respect to the line $E' = 0$. If the level $E'_{\alpha\mu}$ is occupied, the conjugate level with energy $-E'_{\alpha\mu}$ is free, so that in all configurations half the levels are occupied and half are free. At small values of ω in even–even nuclei the ground configuration of the nucleons (ground-state rotational band) corresponds to a diagram with all free levels having positive energy. The excited configurations of an even–even nucleus are obtained by the population of one or several pairs of levels with $E'_{\alpha\mu} > 0$ by quasiparticles and the depopulation of the conjugate levels with $E'_{\alpha\mu} < 0$. The excitation energy with respect to the vacuum of quasiparticles is equal to the sum of the energies $E'_{\alpha\mu}$ occupied by quasiparticles of levels with positive energy. The values of the other additive quantities (such as the angular momentum I, the signature α_t, the number of particles N, and so forth) are calculated similarly, i.e., they are equal to the half-sum of the contributions of all occupied levels, including the levels with positive and negative energy.

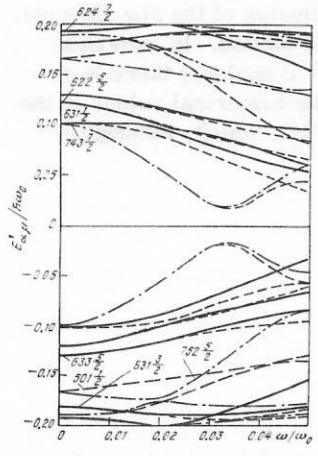

FIG. 14. The same as in Fig. 13 for the neutron levels for N = 143 (Ref. 45); $\lambda = 7.42\hbar\omega_0$, $\varepsilon_2 = 0.24$, $\varepsilon = -0.04$, $\Delta = 0.1\hbar\omega_0$.

In odd nuclei, the vacuum is defined as the lowest configuration with all levels of negative energy occupied (as in even–even nuclei). With this definition, single-quasiparticle states correspond to the lowest configurations of odd nuclei.

When ω increases so much that the levels with positive and negative energy intersect, the definition of the vacuum is changed, and it corresponds to the configuration that describes an even system with minimal total energy of the occupied states. The number of particles in the system is related to the signature of the configuration by $N = 2\alpha_t$ (mod 2); the angular momentum of the states corresponding to the given configuration is constrained by the condition $I = \alpha_t$ (mod 2).

An important property of the diagrams follows from the general relation for the eigenvalues

$$dE/d\omega = \langle \partial H'/\partial\omega \rangle. \tag{32}$$

The right-hand side of Eq. (32) is equal to the quantity $i = \langle \hat{J}_x \rangle$ taken with opposite sign. Thus, the slope of the curves in the diagrams in Figs. 12–14 is equal to the "aligned angular momentum," i.e., to the component of the angular momentum along the x axis:

$$i_{\alpha\mu} = -dE'_{\alpha\mu}/d\omega. \tag{33}$$

Taking literally the postulates of the model of independent quasiparticles, one could assume that the sum of the aligned angular momenta of all the occupied states is equal to the total angular momentum of the state of the nucleus. Such an assumption would be correct if the model were sufficiently accurate for the description of the inertial characteristics of the system as a whole. In view of the possible inaccuracies in the description of the core of the nucleus, phenomenological parameters are usually introduced into the theory to describe the moment of inertia of the core. Bengtsson and Frauendorf[41] have suggested that the core for an even–even nucleus should be determined in accordance with the method of a variable moment of inertia, by introducing the effective moment of inertia

$$J_{\text{core}}(\omega) = I_x(\omega)/\omega = J_0 + \omega^2 J_1. \tag{34}$$

Using an interpolation linear in ω^2 for the moment of inertia of an even–even nucleus at small ω, we can fix the parameters J_0 and J_1. For odd nuclei, the parameters can be determined by choosing the mean values of J_0 and J_1 for the even–even neighbors.

For the energy of the core we then obtain the expression

$$E'_{\text{core}}(\omega) = -\omega^2 J_0/2 - \omega^4 J_1/4 + (1/8)\hbar^2/J_0. \tag{35}$$

The excitation energy of the intrinsic motion in the nucleus, determined in the rotating coordinate system, can be written in the form

$$e'(\omega) \equiv E'(\omega) - E'_{\text{core}}(\omega), \tag{36}$$

where

$$E'(\omega) = [E(I+1) + E(I-1)]/2 - \omega I_x. \tag{37}$$

The experimental values of the angular rotation frequency can be calculated in accordance with

$$\omega(I)=[E(I+1)-E(I-1)]/[I_x(I+1)-I_x(I-1)], \quad (38)$$

in which $E(I+1)$ and $E(I-1)$ are the energies of the adjacent levels of the band with the same value of the signature, and $I_x(I)$ is the "projection of the angular momentum onto the x axis":

$$I_x(I)=\sqrt{(I+1/2)^2-K^2} \quad (39)$$

(K is the angular momentum of the head state of the band).

The expressions in (37) and (36) can be compared directly with experimental data. Such a representation of the experimental data for the state energies of the yrast line of the nucleus ^{184}Os is shown in Fig. 15. The quasiparticle energies $e'(\omega)$ of the states of the ground band are zero because of the felicitous choice of the core; at the same time, the energy of the states of the S band depends strongly on ω and intersects the straight line $e'=0$ at angular frequency $\hbar\omega\approx 0.32$ MeV.

Bohr and Mottelson[40] suggested that the difference

$$i(\omega)=I_x(\omega)-I_{\text{core}}(\omega)\,(I_{\text{core}}(\omega)\equiv\omega J_{\text{core}}(\omega)), \quad (40)$$

should be interpreted as the aligned angular momentum of the intrinsic degrees of freedom of the nucleus. The smooth ω dependence of the moment of inertia determined by Eq. (34) is here taken to describe small admixtures from high-lying configurations of the nucleus. The physical meaning of $i(\omega)$ is revealed by examination of Fig. 16. The ordinary graph representing the anomalous dependence of the moment of inertia on ω^2 is shown in Fig. 16a. The intersection of the bands is reflected in the figure by the sharp increase in the effective moment of inertia. Figure 16b shows how much the values of $I_x(\omega)$ differ for the same values of the angular frequency in the ground-state and S bands. It is this difference that is interpreted as the aligned angular momentum $i(\omega)$ of the S band intersecting the ground-state band (see Fig. 16c).

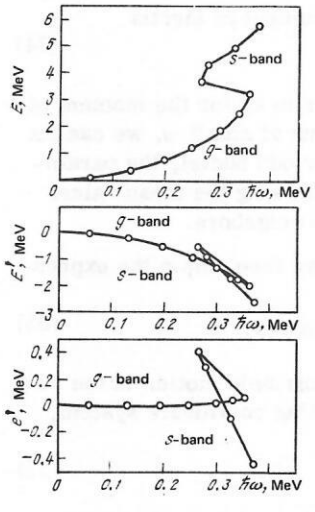

FIG. 15. Dependence on the rotation frequency for the experimental levels of the yrast line of ^{184}Os (E), the levels in the rotating coordinate system found using the data of the experiment (E'), and the quasiparticle energies in the rotating coordinate system (e'). The core parameters are $J_0=24.7$ MeV^{-1} and $J_1=102.9$ MeV^{-3} (Ref. 43).

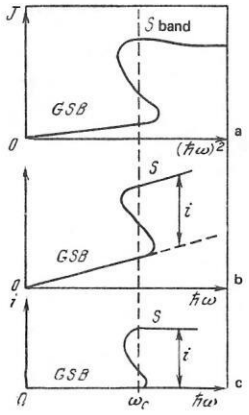

FIG. 16. Schematic representation of intersection of the S band and the ground-state band (i is the aligned angular momentum, and ω_c is the angular rotation frequency at which the crossing occurs).[42]

The example in Fig. 16 shows that the large value of the effective moment of inertia of the S band is caused in the given case precisely by the alignment of the quasiparticle angular momentum. Such a situation is evidently very common, as can be seen from Fig. 17, in which the yrast line of a nucleus is represented schematically as the envelope of parabolas corresponding to collective bands of configurations with values of the aligned angular momentum that increase with increasing spin.

In this connection, it is helpful to recall the discussion about the causes of the anomalous dependence of the effective moment of inertia that arose immediately after the discovery of the effect.[14,46] The earlier interpretation of the anomalous dependence as due to an abrupt change in the pairing and deformation is not correct in the region of spins $\lesssim 15\hbar$, though such effects are manifested at high spins.[47]

A second remark that should be made in connection with the interpretation of the experimental data in terms of an aligned angular momentum relates to the definition of the effective moment of inertia [see the expression (34)]. In the concept of a "core" of a rotating nucleus there is a large degree of uncertainty, this being reflected, naturally, in the estimates of the aligned angular momentum of the intrinsic motion. In individual cases (for example, for the ^{238}U nucleus) there is an uncertainty in the choice of the numerical values of the parameters J_0 and J_1 in Eq. (34), which, although it

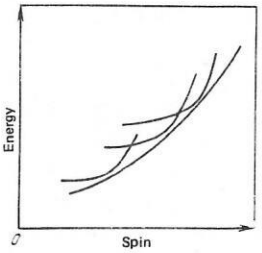

FIG. 17. Schematic representation of the yrast line under conditions of intersection of bands with different values of the aligned angular momentum.

does not affect the qualitative characteristics of $i(\omega)$, does influence the quantitative estimates of the quasiparticle aligned angular momentum. In this connection, it is important that the aligned angular momentum defined by the relations given above is a characeristic very sensitive to the details of the nuclear spectra, and it can therefore be used to determine more precisely the parameters of the microscopic details used to describe nuclear structure.

A physically sounder definition of the core requires particularization of the picture of the nuclear structure. The interpretation of the nuclear states in the framework of the model involving a core and intrinsic excitations coupled to it by the Coriolis forces imposes constraints on the values of the aligned angular momentum in the different bands. Thus, if the core is rigid, the sum of the aligned angular momenta in all bands of a given signature coupled to the core is zero at any fixed value of the angular momentum by virtue of the relation $\mathrm{tr}\,\hat{J}_x = 0$. Such relations can be used in principle for the experimental determination of the inertial properties of the core (of course, provided data are available on the ground-state and S bands of the nuclei). It is hard to imagine grounds for hoping to obtain in this manner an effective moment of inertia equal to the one found in accordance with the prescriptions given above. This conclusion is confirmed by the parametrization of J_{core} using the data on the $K=\frac{1}{2}$ bands based on configurations with small j in the odd Kr nuclei; this differs from the one described above.[48]

The main factor that can lead to a renormalization of the effective moment of inertia is the change in the pairing in the states of an odd nucleus, and also in excited states of even–even nuclei, compared with the pairing in the ground-state band (blocking effect). The consequences of blocking effects were noted in Ref. 49 for ^{171}Hf. Differences between the deformations of neighboring nuclei and also between excited configurations of even nuclei and the ground-state configuration can also lead to a renormalization of the effective moment of inertia. Systematic representation of the data on the ground-state bands of even–even nuclei shows that the parameter J_1 in Eq. (34) depends on the details of the nuclear structure (deformation and/or pairing). It is therefore possible that the renormalization of the effective moment of inertia (the parameter J_1) depends in a complicated manner on the nuclear spin, since different nuclei exhibit appreciable individuality in the way their deformation and pairing change with rotation.

Note that the effective moment of inertia of odd nuclei found from the relations (1) and (2) without allowance for the Coriolis forces systematically exceeds the moment of inertia of the even–even neighbors. However, for bands based on quasiparticle excitations with large j a large fraction of the difference between the effective moments of inertia is due to the Coriolis interaction, which can be taken into account effectively in the cranking model. The validity of this last assertion can be demonstrated by writing down the expression

$$\omega\hat{J}_x = (I/J_{\mathrm{core}})(\hat{R}+\hat{j}_{\mathrm{int}}), \qquad (41)$$

where $\hat{R}$ is the collective angular momentum of the core, and $\hat{j}_{\mathrm{int}}$ is the angular momentum of the intrinsic (quasiparticle) motion. The second part of the expression on the right-hand side of Eq. (41) is the high-spin approximation to the term of the Coriolis interaction from the operator $(\hat{I}-\hat{j}_{\mathrm{int}})2/2J_{\mathrm{core}}$ obtained by the method described in Sec. 1 (see Sec. 3).

Concluding our discussion on the choice of the parameters of the core, we emphasize that the qualitative conclusions about the nuclear structure that follow from analysis of the aligned angular momentum are stable with respect to small variations of the moment of inertia.

The dependence of the aligned angular momentum on ω also contains information on an important characteristic of nuclear structure, namely, the interaction between different configurations. The anomaly in the dependence of the moment of inertia on the rotation frequency (backbending), first explained in Ref. 50 in terms of crossing of the ground-state band and the band of an excited state, is determined by the value $|V|$ of the matrix element of the interaction between the bands. The crossing of the bands is shown schematically in Fig. 18.[51] The distance between the excited bands (broken lines) at the point of intersection of the unperturbed bands (continuous lines) is equal to twice the value $|V|$ of the interaction matrix element (see Fig. 18a). The backbending is shown schematically in Fig. 18b; it begins when there is weak coupling of the bands and takes the form of a sharp rise in the curve of the moment of inertia when the interaction is strong. The condition for occurrence of backbending on intersection of the ground-state band and the S band with aligned angular momentum i_s is the inequality $|V| < i_s^2/4J_c$, where J_c is the moment of inertia of the unperturbed bands at the crossing point.[52]

A systematic study of the variations in the strength of the interaction between the ground-state band and the aligned bands in nuclei of the rare-earth elements was made in Ref. 53 on the basis of Hartree–Fock–Bogolyubov calculations of rotating configurations formed by neutrons of the $i_{13/2}$ shell. These calculations, made for different values of the chemical potential of the neutrons, showed that the absolute magnitude of the matrix element of the interaction oscillates as a function of the number of neutrons and has five zeros, in the region of which one can expect to discover backbending.

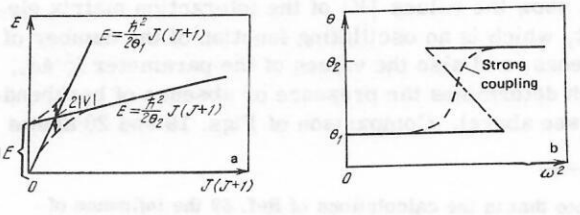

FIG. 18. Dependence of the energy on the spin for the levels of the intersecting ground-state band and S band (a) and the dependence on ω^2 of the effective moment of inertia of the yrast line of the nucleus (b).[51] The chain line corresponds to weak interaction with the anomalous dependence on the rotation frequency typical of backbending; the broken curve corresponds to strong interaction of the bands.

Cranking-model calculations for the nuclei of rare-earth elements have been made in a large number of publications.[54-58] Bengtsson and Frauendorf[41,52] analyzed the available experimental data in this region of nuclei and compared the information on the strength of the interaction of the bands deduced from the experimental data with the results of the theoretical study. This comparison showed that the cranking model agrees qualitatively with the experiments. The theory presented in the quoted studies can hardly pretend to complete quantitative correspondence with experiment, since it does not take into account the change with rotation in the gap of the pairing correlations and the deformation, but it does reproduce well the experimentally observed oscillations in the strength of the interaction between the bands of the nuclei of the rare-earth elements. More complicated calculations, which introduce corrections for not only the nucleons in the $i_{13/2}$ levels but also the core nucleons and also take into account exactly the conservation of the particle number and the angular momentum, were published in Ref. 51.

In the region of the actinides, the calculations revealed the presence of the following interesting feature. As can be seen from Figs. 13 and 14, the values of the rotation frequency ω_c at which the levels above and below the Fermi surface cross are almost the same for the proton and neutron components. This is due to the compensation of two effects. The proton level nearest the Fermi surface is the level $i_{13/2}, K=5/2$, whereas the analogous neutron level belongs to the $j_{15/2}$ shell but has K number equal to $7/2$. The smaller K of the proton level should lead to a more rapid alignment, which is compensated by the larger value of the j number of the neutron level. Cranking-model calculations[59] similar to those described above[41,52] lead to a number of predictions for nuclei in the actinide region.[2)] The results of these calculations are shown in Figs. 19 and 20.

Figures 19 and 20 show the first three intersections of the levels of the $i_{13/2}$ proton and $j_{15/2}$ neutron shells. The first crossing of the levels can be observed in the sequence of yrast levels resulting from intersection of the ground-state rotational band of the even–even nuclei with the two-quasiparticle S band; the other two intersections can be manifested in the spectra of the odd nuclei, when the first intersection is blocked by the Pauli principle. In this case, the two branches of the band of the ground-state configuration of an odd nucleus ($\alpha=\pm\frac{1}{2}$) intersect three-quasiparticle configurations. The figures show the values $|V|$ of the interaction matrix element, which is an oscillating function of the number of nucleons, and also the values of the parameter $i_s^2/4J_c$, which determines the presence or absence of backbending (see above). Comparison of Figs. 19 and 20 shows

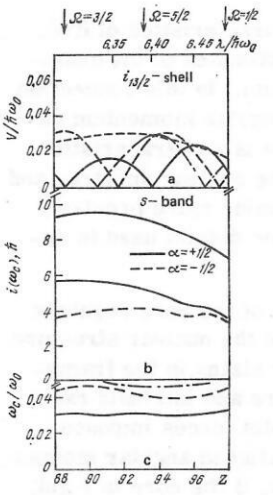

FIG. 19. Dependence on Z of the rotation frequency ω_c at the points of the first crossing of the levels (continuous curve) and the following two levels (broken curve for $\alpha=\frac{1}{2}$ and chain curve for $\alpha=-\frac{1}{2}$) for the $i_{13/2}$ proton levels (c); the dependence of the corresponding values $|V|$ of the interaction matrix element (a) and the aligned angular momentum $i(\omega_c)$ of the quasiparticle in the levels participating in the first crossing (b).[59]

that the rotation frequencies at the points of intersection of the proton and neutron levels are very close to each other. The alignment in the neutron S configuration is somewhat less than in the proton configuration, which is confirmed by the analysis of the experiment described below (see Fig. 21).

It should be noted that in the actinides, in which the moment of inertia J_c is relatively large compared with the nuclei of the rare-earth elements, while the values of the aligned angular momentum i are approximately the same, the limiting value $V=i_s^2/4J_c$ for backbending is numerically rather small. Therefore, backbending must be observed rather seldom in the actinide nuclei. The arguments given in Ref. 59 show that the limiting values given in Figs. 19 and 20 are overestimated, so that, for example, in the nuclei of Th, U, and Cm one must expect a monotonic increase in the moment of in-

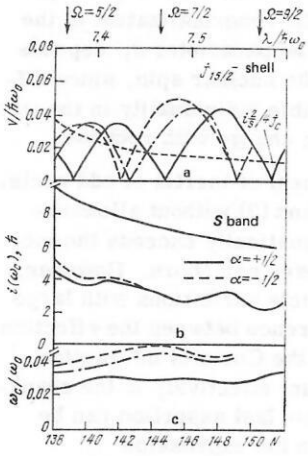

FIG. 20. Dependence of the curves analogous to Fig. 19 for the $j_{15/2}$ neutron system on the number of neutrons N.[59]

[2)] Note that in the calculations of Ref. 59 the influence of rotation on the characteristics of the nuclear field are ignored, and the deformation, gap parameter Δ, and chemical potential are kept unchanged in the calculations. However, allowance is made for the decrease in Δ due to the blocking effect. The parameter Δ is decreased by 20% compared with the value determined from the odd–even mass difference.

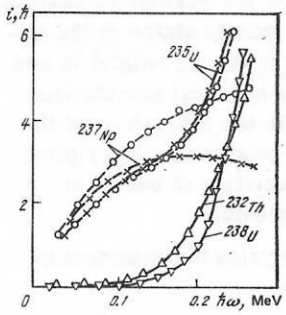

FIG. 21. Alignment of the angular momentum in the yrast states of the odd-proton nucleus ^{237}Np and the odd-neutron nucleus ^{235}U up to the spin value $I = 57/2$ in comparison with the neighboring even–even nuclei ^{232}Th and ^{238}U ($I \leqslant 30\hbar$). The core parameters for ^{237}Np are $J_0 = 66.9\ \hbar^2/\text{MeV}$, $J_1 = 306\ \hbar^4/\text{MeV}^3$; for ^{235}U, $J_0 = 67.3\ \hbar^2/\text{MeV}$, $J_1 = 354\ \hbar^4/\text{MeV}^3$; for ^{232}Th, $J_0 = 60.4\ \hbar^2/\text{MeV}$, $J_1 = 429\ \hbar^4/\text{MeV}^3$; for ^{238}U, $J_0 = 66.6\ \hbar^2/\text{MeV}$, $J_1 = 380\ \hbar^4/\text{MeV}^2$.

ertia in the region of intersection of the configurations (backbending can be expected in the nuclei of Ra and Pu). A monotonic dependence of the moment of inertia on ω can also be expected in the majority of the neutron yrast lines, except for $N \approx 138$–140 and $Z = 144$. These features make it possible to interpret the proton and neutron configurations of deformed nuclei at the beginning of the actinide region.

Figure 21 shows the results of analysis of experimental data in terms of an aligned angular momentum in yrast configurations of the nuclei ^{237}Np and ^{235}U (Refs. 23, 33, and 34) and also in the neighboring even–even nuclei ^{232}Th and ^{238}U. As can be seen from the figure, the rotational alignment in the proton $i_{13/2}$ configuration increases rapidly at low rotation frequencies. For $\hbar\omega \gtrsim 0.1$ MeV, the increase in the aligned angular momentum becomes slower first in the branch $\alpha = -\frac{1}{2}$ and then in the branch $\alpha = +\frac{1}{2}$ and virtually ceases when $\hbar\omega \gtrsim 0.18$ MeV. The core parameters were determined by averaging the data over the ground-state bands of the neighboring even–even nuclei:

$$J_0 = 66{,}9\hbar^2/\text{MeV},\ J_1 = 306\hbar^4/\text{MeV}^3.$$

An odd-neutron case (^{235}U) is represented by the second pair of curves in Fig. 21. At small ω, the branches with different values of the signature virtually coincide. This is due to the fact that compared with ^{237}Np there is a much smaller admixture of the component of the level $j_{15/2}\Omega = \frac{1}{2}$, which at small ω determines the difference between the two branches, in the ground-state configuration of ^{235}U ($7/2^-[743]$). However, at large values of ω the branches clearly diverge. In the region $0.12\ \text{MeV} \leqslant \hbar\omega \leqslant 0.18$ MeV there is saturation, after which there follows a rapid growth of i, which begins at $\hbar\omega \approx 0.18$ MeV. The core of the neutron system was determined by the weighted mean of the parameters for ^{232}U and ^{236}U in order to eliminate from the determination of the core the effects of the strong interaction of the configurations in ^{234}U, which lead to a local maximum in the value of the parameter J_1. The values of the inertial parameters of ^{235}U used in plotting the figure are

$$J_0 = 67{,}3\hbar^2/\text{MeV},$$
$$J_1 = 354\hbar^4/\text{MeV}^3.$$

The additional alignment of the angular momentum in ^{235}U at $\hbar\omega \approx 0.18$ MeV is due to the interaction of the ground-state band and the proton S band (because of the Pauli principle, the neutron in the state $7/2^-[743]$, which determines the yrast configuration of ^{235}U, blocks the neutron S level). From the data on the aligned angular momentum in the intermediate region of $\hbar\omega$, in which saturation of the aligned angular momentum of the $i_{13/2}$ configurations is noted, it can be concluded that the intersection of the configurations occurs at the frequency $\hbar\omega \approx 0.25$ MeV ($i_c \approx 7\hbar$), in accordance with the theoretical estimates described earlier.

Figure 21 shows the values of the aligned angular momentum in the nuclei ^{238}U and ^{232}Th. In ^{238}U, the dependence $i(\omega)$ is very close to that given by the proton alignment in ^{235}U. This observation confirms the conclusion that the first crossing in the light actinides is associated with the proton S band, as is indicated by the fact that the curves of the aligned angular momentum in ^{237}Np at these values of the rotation frequency still manifest saturation.

Besides ^{232}Th and ^{238}U, the spectra of the nuclei ^{234,236}U (Ref. 37) and ^{248}Cm (Ref. 38) at high spins were studied. In none of these cases was backbending observed, and the curves of the effective moment of inertia increase monotonically as functions of the square of the rotation frequency (Fig. 22). As we noted above, this indicates a strong interaction of the configurations. The curves of the aligned angular momentum in the even–even nuclei indicate that the frequencies of the crossing of the proton and neutron S bands and the ground band are very nearly equal (this is indicated, for example, by the absence of saturation in the very last states of the nuclei ^{232}Th and ^{238}U shown in Fig. 21, in which the proton configurations contribute approximately $6\hbar$ to the aligned angular momentum). In ^{237}Np, additional alignment is not observed up to $\hbar\omega \approx 0.28$ MeV, which can be interpreted as due to the weak interaction of the bands predicted by theory (see Figs. 19 and 20); for in the case of weak interaction of the bands, Coulomb excitation leads to population of levels of the ground band after the crossing point, and the corresponding levels of the yrast band are not manifested.

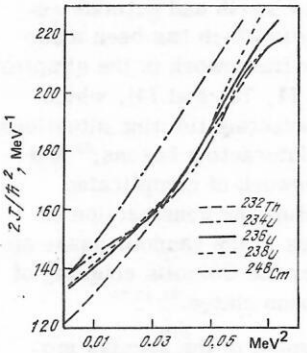

FIG. 22. Dependence of effective moments of inertia of some nuclei in the region of the actinides on $(\hbar\omega)^2$.[37]

3. ALIGNMENT OF THE ANGULAR MOMENTUM OF OCTUPOLE VIBRATIONS OF EVEN-EVEN DEFORMED NUCLEI

At the lowest values of the angular momentum, the negative-parity rotational bands in deformed nuclei can be put schematically into two categories—octupole vibrational bands and two-quasiparticle bands. Collective effects in negative-parity states have been studied since about 1963.[60,61] A large degree of collectivization of the states $K^\pi = 0^-, 1^-, 2^-$ was found as a result of calculations in the random-phase approximation.[60-62]

The octupole vibrations are characterized by low values of the excitation energy; they do not strongly influence the inertial properties of the nuclei, so that the moment of inertia of the core in octupole states is approximately the same as in the states of the ground band (see below). At low spins, the two-quasiparticle states have a higher excitation energy, but because of the blocking effect and the alignment of the quasiparticle angular momentum, which may be very appreciable, there are among such states some with significantly larger moments of inertia than is the case for the states of the ground band. With increasing angular momentum, the intrinsic angular momenta of the vibrational and quasiparticle motion tend to become aligned along the direction of the collective rotational angular momentum to decrease the kinetic energy of the rotation by virtue of the potential energy of the coupling of the intrinsic motion to the average field of the rotating core.

The effects of the coupling to the rotation have a strong influence on all the properties of the octupole vibrational states. The Coriolis coupling of the octupole bands is strong on the scale of the difference between the excitation energies of the octupole vibrational states with different values of K already at very moderate values of the total angular momentum.[63,64] Therefore, alignment of the vibrational angular momentum in the negative-parity bands begins earlier than the alignment of the intrinsic angular momentum associated with the quasiparticle motion. However, at high angular momentum the two-quasiparticle degrees of freedom are also activated by the Coriolis forces.

At the present time, there is extensive experimental (Refs. 25–28 and 66–70) and theoretical (Refs. 63–65 and 71–75) material on the negative-parity rotational bands in the nuclei of the rare-earth and actinide regions. The theoretical analysis which has been made includes investigations in the framework of the simplest collective models (Refs. 63, 71, 73, and 74), which make it possible to study interesting limiting situations, calculations in the model of interacting bosons,[68] and also calculations in the framework of complicated microscopic schemes, including the construction of phonons of a deformed nucleus in the random-phase approximation and allowance for the Coriolis coupling of a large number of single-phonon states.[65,72,75]

We describe here the alignment of the angular momentum in negative-parity bands in the framework of a very simple phenomenological model.[76] As will be shown later, this model explains the qualitative changes in the structure of the negative-parity states in the nuclei of the actinide region, and it is also helpful in considering the results of more fundamental calculations based on microscopic theory. In the discussion of the results, much attention will be paid to the description of the electromagnetic characteristics of nuclei in states with aligned angular momentum.

Phenomenological model for analyzing the alignment of the octupole angular momentum.

We consider the model of a nucleus with the Hamiltonian[76]

$$\hat{H} = a \sum_{i=1}^{3} (\hat{J}_i - \hat{j}_i)^2 + \hat{\mathcal{H}}_{\text{intr}}, \tag{42}$$

where $\hat{J}_i$ and $\hat{j}_i$ $(i = 1, 2, 3)$ are, respectively, the projections of the total and the vibrational angular momentum onto the intrinsic axes of the nucleus, $a = J/2$ is the inertial parameter which characterizes the core of the deformed nucleus, and, finally,

$$\hat{\mathcal{H}}_{\text{intr}} = \sum_{|K| \leqslant \lambda} \omega_{|K|} b^+_{\lambda K} b_{\lambda K} \tag{43}$$

is the intrinsic part of the Hamiltonian, which describes the phonon excitations. The phonon operators in (43) carry the indices λ and K, which determine their transformation properties with respect to rotations of the intrinsic coordinate system. We assume that the transformation properties of the phonons are identical with those for tensors of rank λ. We have the commutation relations

$$\begin{aligned} [\hat{j}_3,\ b^+_{\lambda K}] &= K b^+_{\lambda K}; \\ [\hat{j}_\pm,\ b^+_{\lambda K}] &= \sqrt{(\lambda + 1/2)^2 \mp (K + 1/2)^2}\, b^+_{\lambda K \pm 1}. \end{aligned} \tag{44}$$

The situation described by the Hamiltonian (42)–(44) corresponds to a nucleus with stable deformation of the axial symmetry and phonon degrees of freedom not distorted by the deformation. The intrinsic Hamiltonian defined in accordance with (19) has in the considered case the form

$$\hat{H}^I_\xi = aI(I+1) - 2aI\hat{j}_1 + \hat{\mathcal{H}}_{\text{intr}}. \tag{45}$$

To analyze H^I_ξ, it is convenient to go over to the representation in which the operator of the projection of the angular momentum onto the rotation axis is diagonal:

$$(\hat{j}_1)_{\tau\tau'} = \tau\delta_{\tau\tau'} \quad (-\lambda \leqslant \tau \leqslant \lambda). \tag{46}$$

In what follows, we shall call this representation the τ representation, distinguishing it from the K representation, in which the intrinsic Hamiltonian is diagonal [see Eq. (43)]. The transition from the K representation to the τ representation is made by a rotation of the intrinsic coordinate system through angle $\pi/2$ around the second intrinsic axis. This gives

$$(\hat{\mathcal{H}}_{\text{intr}})_{\tau\tau'} = \sum_{K \geqslant 0} d^\lambda_{K\tau}\left(\frac{\pi}{2}\right) d^\lambda_{K\tau'}\left(\frac{\pi}{2}\right) \frac{\omega_K\,(1 + (-1)^{\tau+\tau'})}{(1 + \delta_{K,0})}, \tag{47}$$

where $d^\lambda_{K\tau}(\pi/2)$ is the average part of the D function at $\theta = \pi/2$ (see Ref. 79, p.109 of Russian translation). Equation (47) shows that $\hat{\mathcal{H}}_{\text{intr}}$ and, with it, H^I_ξ have block-diagonal structure, only the intrinsic states for

which the parity of the quantum number τ is the same being mixed. Noting that on rotation around the first axis through π the phonon operator

$$b^{\dagger}_{\lambda\tau} = \sum_{K} d^{\lambda}_{K\tau} \left(\frac{\pi i}{2}\right) b^{\dagger}_{\lambda K} \tag{48}$$

acquires a phase equal to $(-1)^{\tau}$, we see that the signature quantum number discussed earlier is indeed conserved in the given approximation. Accordingly, states with different signature can be analyzed independently.

We now turn to the description of the alignment of the octupole vibrational angular momentum. The octupole vibrations correspond to $\lambda = 3$. The model of octupole bands with Hamiltonian defined above is very close as regards its physical content to the model described in Ref. 71.

The block of the Hamiltonian matrix corresponding to the positive-signature states contains matrix elements coupling the basis states $\tau = 0, \pm 2$. This part of the Hamiltonian can be represented in the form

$$(H^{I}_{\xi})_{+} = aI(I+1) + \begin{pmatrix} -4aI + \mathcal{H}_{22} & \mathcal{H}_{20} & \mathcal{H}_{2-2} \\ \mathcal{H}_{20} & \mathcal{H}_{00} & \mathcal{H}_{20} \\ \mathcal{H}_{2-2} & \mathcal{H}_{20} & 4aI + \mathcal{H}_{22} \end{pmatrix}, \tag{49}$$

where

$$\left.\begin{aligned} &\mathcal{H}_{2\pm2} = (3/16)\,\omega_3 \pm (8/16)\,\omega_2 + (5/16)\,\omega_1; \\ &\mathcal{H}_{20} = (1/8)\sqrt{15/2}\,(\omega_3 - \omega_1); \\ &\mathcal{H}_{00} = (5/8)\,\omega_3 + (3/8)\,\omega_1. \end{aligned}\right\} \tag{50}$$

The Hamiltonian matrix corresponding to the negative-signature states has the form

$$(H^{I}_{\xi})_{-} = aI(I+1) + \begin{pmatrix} -6aI + \mathcal{H}_{33} & \mathcal{H}_{31} & \mathcal{H}_{3-1} & \mathcal{H}_{3-3} \\ \mathcal{H}_{31} & -2aI + \mathcal{H}_{11} & \mathcal{H}_{1-1} & \mathcal{H}_{3-1} \\ \mathcal{H}_{3-1} & \mathcal{H}_{1-1} & 2aI + \mathcal{H}_{11} & \mathcal{H}_{31} \\ \mathcal{H}_{3-3} & \mathcal{H}_{3-1} & \mathcal{H}_{31} & 6aI + \mathcal{H}_{33} \end{pmatrix}. \tag{51}$$

Here

$$\left.\begin{aligned} &\mathcal{H}_{3,\pm3} = (1/32)\,\omega_3 \pm (3/16)\,\omega_2 + (15/32)\,\omega_1 \pm (5/16)\,\omega_0; \\ &\mathcal{H}_{3,\pm1} = (\sqrt{15}/32)\,[\omega_3 - \omega_1 \pm 2(\omega_2 - \omega_0)]; \\ &\mathcal{H}_{1,\pm1} = [15\omega_3 + \omega_1 \pm 2(5\omega_2 + 3\omega_0)]/32. \end{aligned}\right\} \tag{52}$$

From the Schrödinger equation

$$(\mathcal{H}^{I}_{\xi})_{\sigma}\,\psi_{\sigma\lambda} = E^{I}_{\sigma\lambda}\psi_{\sigma\lambda} \tag{53}$$

for the energy eigenvalues $E^{I}_{\sigma\lambda}$ of the states and the eigenvectors

$$\psi_{+} = \begin{pmatrix} \psi_2 \\ \psi_0 \\ \psi_{-2} \end{pmatrix}; \quad \psi_{-} = \begin{pmatrix} \psi_3 \\ \psi_1 \\ \psi_{-1} \\ \psi_{-3} \end{pmatrix} \tag{54}$$

we obtain an equation for determining $E^{I}_{\sigma\lambda}$ in the form

$$F_{I,\sigma}(E^{I}_{\sigma\lambda}) = 0, \tag{55}$$

where $F_{I,\sigma}(x)$ are polynomials of third ($\sigma = +$) or fourth ($\sigma = -$) order whose solution can be written down in analytic form.[79]

In the following exposition, we shall restrict ourselves to the special case when

$$\omega_1 = \omega_2 = \omega_3 = \omega_0 + \Delta. \tag{56}$$

Many interesting conclusions can be obtained even with this economic parametrization of the Hamiltonian. The main tendencies in the development of the alignment can be revealed by considering the quasidegenerate case (56) even in the cases when (56) is not satisfied identically. On the other hand, the case (56) provides the possibility of a very complete analysis of physical phenomena, since the solutions of the equations depend in this case on only the single variable $\chi = aI/\Delta$.

When (56) is satisfied, the matrix of the Hamiltonian $(\mathcal{H}^{I}_{\xi})_{+}$ is diagonal in the τ representation. Therefore, the projection of the angular momentum onto the rotation axis is an exact quantum number in the framework of this model. The energies of the positive-signature states are determined by the formula

$$E_{+,\tau}(I) = \omega_0 + \Delta + a[R(R+1) - \tau(\tau-1)], \tag{57}$$

where $R = I - \tau$ is the collective rotational angular momentum. The aligned angular momentum in such states is $\tau \equiv \langle \hat{j}_i \rangle (\tau = 0, \pm 2)$. As follows from Sec. 1, the total angular momentum in the positive-signature states takes even values (together with R). It can be seen from (57) that the lowest positive-signature band is similar to the ground-state rotational band shifted by two Planck units in the angular-momentum scale and raised by $\omega_0 + \Delta - 6a$ in energy.

Odd values of the angular momentum I correspond to the negative-signature states. The energies of such states can be determined from the expression

$$E_{-,\lambda}(I) = \omega_0 + aI(I+1) + \Delta\chi\varepsilon_{\lambda}(\chi), \tag{58}$$

in which $\varepsilon_{\lambda}(\chi)$ are solutions of the equations

$$\left.\begin{aligned} &z\{z\{z(z - 1/\chi\} - 40\} + 16/\chi\} + 144 = 0, \\ &z = 1/\chi - \varepsilon. \end{aligned}\right\} \tag{59}$$

The solutions of (59) determine four families of states; the dependence $\varepsilon_{\lambda}(\chi)$ for these solutions is shown in Fig. 23. The lowest of these curves corresponds to the $K^{\pi} = 0^{-}$ octupole vibrational band distorted by the coupling between the rotation and the vibrations. At small values of the angular momentum ($\chi \ll 1$), the states of this band have excitation energies approximately equal to $E^{-}_{0}(I) = \omega_0 + aI(I+1)$. At high spins ($\chi \gg 1$), $\varepsilon_{\min} \approx -6$ and for the energies of this band we obtain the expression $E(I) = \omega_0 + a(I + \frac{1}{2} - 3)^2$, from which it follows that this family of states in the limit of large spins is transformed into a family of states with vibrational angular momentum directed along the collective rotational state, i.e., in the completely aligned state. The other

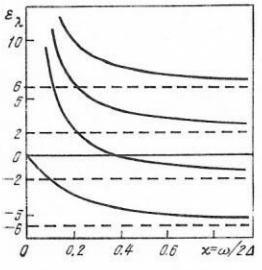

FIG. 23. Solutions of (59) for $\varepsilon_{\lambda}(\chi)$, which determine the energies of the octupole states of negative signature.

solutions of (59) correspond to rotational bands whose excitation energy at small I is $\omega_0+\Delta$. Because of the degeneracy [see Eq. (56)], these bands cannot be given a definite K number even at low spins.

If the angular momentum is large, the energy intervals between neighboring states belonging to the same family can be approximated by the expression

$$E_\lambda(I+1)-E_\lambda(I-1)\equiv\delta E_\lambda(I)$$
$$\approx 2\,dE(I)/dI=2\omega_\lambda^{\mathrm{rot}}(I). \qquad (60)$$

As we said above, $\omega_\lambda^{\mathrm{rot}}(I)$ is the angular frequency of rotation of a nucleus in state λ with angular momentum I.

Since E_λ^I is an eigenvalue of the Hamiltonian H_ξ^I, we have[80]

$$\frac{dE_\lambda}{dI}=\left\langle\psi_\lambda\left|\frac{\partial H_\xi^I}{\partial I}\right|\psi_\lambda\right\rangle=2a\,[(I+1/2)-j_x^\lambda], \qquad (61)$$

where

$$j_x^\lambda=\langle\psi_\lambda|\hat{j}_1|\psi_\lambda\rangle \qquad (62)$$

is the projection of the vibrational angular momentum onto the rotation axis. Determining the moment of inertia $J_\lambda=1/2a$ of the core and using Eq. (60), we write the relation (61) in the form

$$j_x^\lambda=I+1/2-\omega_\lambda^{\mathrm{rot}}(I)\,J_\lambda. \qquad (63)$$

This expression is identical to the one used in Sec. 2 to analyze the alignment of the quasiparticle angular momentum in odd nuclei. The generality of Eq. (63) is obvious—it is valid for any model in which the I dependence of the operator H_ξ^I is determined by Eq. (46).

The aligned vibrational angular momentum j_x^λ can be calculated in the framework of our model either by differentiating the energy E_λ^I with respect to I,

$$j_x^\lambda=-\frac{1}{2}\frac{d}{d\chi}[\chi\varepsilon_\lambda(\chi)], \qquad (64)$$

or by finding the expectation value of $\hat{j}_1$ in accordance with (62). The χ dependence of j_x^λ for four branches of negative-signature octupole states is shown in Fig. 24. In the limit of large χ (large values of I), j_x^λ approaches asymptotically the values 3, 1, −1, −3 for the branches with energies $\varepsilon_1<\varepsilon_2<\varepsilon_3<\varepsilon_4$, respectively. As we have already noted, the 0^- rotational band is transformed at large I into a band with completely aligned octupole angular momentum ($j_x\to 3$). The vibrational angular momentum remains only partly aligned along the rotation axis in the states of other bands even at high angular momenta. The limiting value of the aligned angular momentum in the band is equal to the τ value of the component of the wave function whose weight is predominant at high angular momenta. The structure of the wave vector ψ [see Eq. (54)] for the states of the 0^- band is shown as a function of χ in Fig. 25. As can be seen from Figs. 24 and 25, the values of j_x^λ and ψ_τ are very close to their limiting values even for $\chi=0.5$ ($I=J_\lambda\Delta$). For this value of χ, $j_x=2.73$ and $\psi_{\tau=3}=0.904$ in the lowest octupole band.

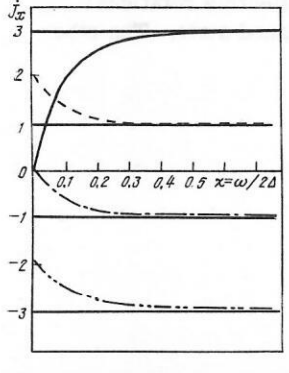

FIG. 24. Aligned vibrational angular momentum of single-phonon octupole states of negative signature.

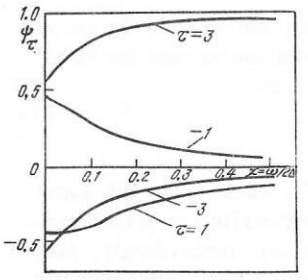

FIG. 25. Dependence of structure of the wave function of the states of the lowest octupole band in the τ representation on the rotation parameter $\chi=aI/\Delta$.

Analysis of the spectrum of the 0^- band in the actinides

Study of the negative-parity rotational bands in the actinides is of particular interest in connection with the fact that in these nuclei the activation by rotation of the two-quasiparticle states becomes important at rather large angular momenta ($I\approx 20$), whereas the rotational coupling of the collective bands is manifested much earlier.[65,77] Therefore, the alignment of the vibrational angular momentum must be manifested rather clearly. On the other hand, it has recently become possible to obtain fairly extensive experimental information about the spectra of the 0^- bands in the nuclei of this region (Refs. 25, 27, 28, 66, and 67).

The existence of coupling between the rotation and the octupole vibrations in the nuclei is clearly shown in diagrams like those given in Fig. 26 (Ref. 27) (the adiabatic limit of the octupole band of a rigid rotator is shown in the figure by the broken curves). Complete alignment of the octupole angular momentum in the nuclei of the actinide region corresponds to spins $I\gtrsim 10$–15. Judging from the positions of the experimental points, the asymptotic behavior of the large angular momenta in the nuclei ^{232}Th and ^{236,238}U is distorted by effects other than alignment of the octupole angular momentum.[72]

A clearer picture of the changes in the structure of nuclei when the angular momentum of the state is increased can be obtained by studying the dependence on the angular frequency of the rotation of the core for the aligned angular momentum found in accordance with Eqs. (60) and (63). In constructing graphs of the aligned angular momentum, it is necessary to make assumptions about the moment of inertia J_λ of the core.

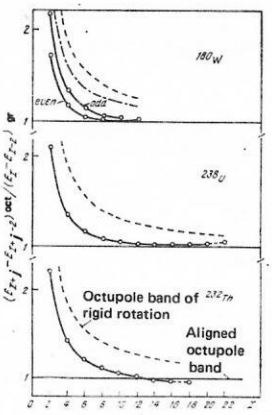

FIG. 26. Ratio of the energy intervals between the states of the aligned octupole band and the g band in three nuclei (^{180}W, $K^{\pi}=2^-$ band, $j=2$; ^{238}U and ^{232}Th, $K^{\pi}=0^-$ band, $j=3$).[27] The limiting situations of adiabatically slow rotation and complete alignment of the octupole angular momentum along the rotation axis are shown.

The usual choice of J_λ corresponds to a fitting by means of the Harris formula of the first two levels of the ground-state band of the considered nucleus (see Sec. 2). For comparison with the phenomenological model considered above, it is convenient to use instead of the angular frequency of the rotation the quantity

$$\chi=\omega_\lambda^{\mathrm{rot}}/2\Delta;\ \Delta=(\omega_1+\omega_2+\omega_3)/3-\omega_0. \tag{65}$$

An example of such a construction is shown in Fig. 27, in which we have plotted the angular momentum in the 0^- band of ^{238}U. The experimental data used in the construction of Fig. 27 and the following figures in this section are taken from Refs. 27 and 28. The parameters J_0 and J_1, which determine the moment of inertia and the value of the parameter Δ, are shown in the figure. The chosen value of Δ corresponds to the positions of the head states of the octupole bands, and it was determined in Ref. 75 using the conditions of best description of the experimental energies of the 0^- band in the framework of a microscopic model. It can be seen from the figure that the simple model is capable of describing fairly well the alignment of the angular momentum in a wide range of spins. Figure 27 also shows the "aligned angular momentum" in the ground-state band, which determines the part played by the intrinsic excitations of the core. It can be seen that a

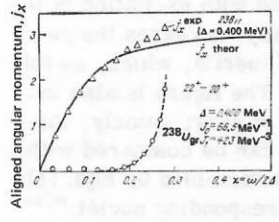

FIG. 27. Aligned angular momentum in 0^- band of ^{238}U determined using the data of Refs. 27 and 29. The continuous curve is plotted using the equations of the model described in the text. The "experimental" points are obtained by the method of Ref. 52 using the parameters J_0 and J_1 given in Fig. 21. The broken curve shows the "aligned angular momentum" in the yrast configuration calculated in the same scheme.

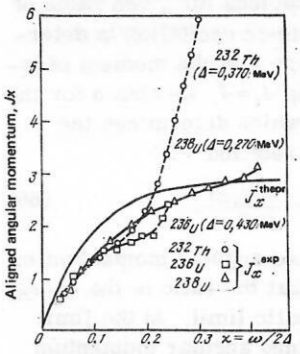

FIG. 28. The same as in Fig. 27 for the nuclei ^{232}Th, ^{236}U, and ^{238}U. The experimental data for ^{236}U are taken from Ref. 37. The parameter Δ for each of the nuclei is determined using the data of the calculation of the head states of the negative-parity bands in the quasiboson approximation.[81]

discrepancy between the theory and experiment in the description of the 0^- band arises in the region of angular momenta in which excitation of the core becomes important.

More systematic information about the aligned angular momentum in the 0^- band of actinide nuclei is contained in Fig. 28. Fitting parameters were not used in the construction of the figure. The inertial parameters of the core were found from the excitation energies of the lowest states of the ground-state band of the corresponding nucleus. The parameter Δ was determined in accordance with Eq. (65) from the excitation energies of the states $K^-=0^-,1^-,2^-,3^-$ calculated in the framework of the microscopic theory.[81] The change in Δ compared with the values used in Fig. 27 has influenced the agreement between experiment and the phenomenological model. At low spins, the aligned angular momentum in all three nuclei follows a more or less universal dependence on χ. However, the simple phenomenological model predicts a larger value of the aligned angular momentum than follows from experiment. It can be said that the nuclei represented in Fig. 28 exhibit a weakening of the Coriolis mixing of the negative-parity states compared with the limit of "spherical" octupole phonons. Such a phenomenon could be expected from the observations as a measure of the collectivization of the lowest K^- states; indeed, random-phase calculations[60,62,81] indicate that the lowest 3^- states are hardly collectivized at all, i.e., that the "spherical" 3^- phonon either fragments over states in a wide range of excitation energies or is raised high above the Fermi surface.

In the region of angular momenta corresponding to $\chi \approx 0.25$ ($\omega_\lambda^{\mathrm{rot}} \approx 0.15$–$0.20$ MeV), the experimental points begin to depart rapidly from the theoretical curve. This region of angular frequencies is only slightly shifted to values of ω^{rot} lower than the value at which excitation of the core is manifested in the alignment of the quasiparticle angular momentum in odd nuclei in the region of the actinides (see Sec. 3).

The information about the aligned angular momentum contained in Figs. 26 and 28 is essentially the same. This follows directly from Eqs. (60) and (61). The an-

gular rotation frequency of a nucleus for given value of the spin in a state without intrinsic excitation is determined by Eqs. (1) and (2), where J is the moment of inertia for the yrast line. Setting $J_\lambda = J$, we obtain for the ratio of the energy intervals, which determines the function shown in Fig. 26, the relation

$$\left\{\frac{(E(I+3)-E(I+1))_{\text{oct}}}{(E(I)-E(I-2))_{\text{gr}}}-1\right\}2J\Delta=\frac{3-j_x(\chi)}{\chi}. \qquad (66)$$

At small values of χ, the aligned angular momentum in the 0^- band tends to zero, so that the ratio of the energy intervals approaches the adiabatic limit. In the limit of high spins ($\chi \gtrsim 0.5$), the aligned angular momentum approaches three Planck units, and the quantity in the numerator on the right-hand side of Eq. (66) tends to zero.

The function $[3-j_x(\chi)]/\chi$ calculated in accordance with the equations of the previous section is compared in Figs. 29 and 30 with the experimental data for ^{238}U and ^{232}Th. As we mentioned above, the determination of the aligned angular momentum j_x^{exp} involves hypotheses about the inertial parameters of the ground-state band. The employed parametrization of the moment of inertia does not ensure exact reproduction of the energy intervals in the yrast band. In contrast, at large angular momenta the deviations of $[E(I)-E(I-2)]_{\text{gr}}^{\text{exp}}$ from the value calculated by the Harris formula become appreciable. As a result of this, the calculation of the experimental values of the right- and left-hand sides of Eq. (66) gives different results, the difference beginning to increase rapidly in the region of spins in which the Harris formula does not approximate well the spectrum of the yrast band. However, in the region of angular momenta up to about $(11-13)\hbar$ the simple model described above reproduces fairly well the experimental situation as reflected by the diagrams in Figs. 26, 29, and 30. This was already noted in Ref. 76.

In the preceding discussion, the question of determining the moment of inertia of the core arose several times. In the Bengtsson–Frauendorf theory[41,52] and the phenomenological model considered here, this problem is solved more or less arbitrarily by using data on the ground-state rotational band and the assumption of a smooth dependence of the angular momentum of the core

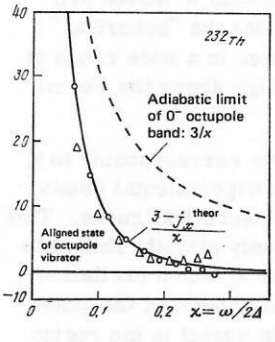

FIG. 29. Dependence of the ratio of the energy intervals shown shown in Fig. 26 on the rotation parameter $\chi = \omega/2\Delta$. The continuous curve shows $(3-j_x(\chi)/\chi)$ constructed using the equations of the model; the open circles show $(3-j_x(\chi))^{\text{exp}}/\chi^{\text{exp}}$, the open triangles $2J_{\text{gr}}\Delta\{\delta E_{\text{oct}}^{\text{exp}}/\delta E^{\text{exp}}-1\}$; $\Delta = 0.4$ MeV.

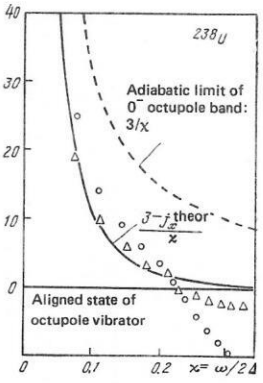

FIG. 30. The same as in Fig. 29 for ^{232}Th. The parameters are the same as in Fig. 28.

on the angular frequency of rotation. For a better justified choice of the inertial parameters of the core, we need more complete information than the spectrum of one band of the nucleus. This circumstance is very clearly manifested in the description of the negative-parity states in the framework of the model described earlier. We have already seen that the description of the experimental data on the energies of the yrast-band states depends strongly on the choice of the energy interval Δ between the bands (cf. Figs. 27 and 28).

Since all physical quantities can be expressed in the framework of the model by functions of the one variable $\chi = (I+\frac{1}{2})/(2\Delta J_\lambda)$, the choice of J_λ also influences the relationship between the theoretical and experimental data. One can determine J_λ in such a way that the spectrum of the 0^- band is exactly described by the formulas of the present model. For this, it is necessary to write Eq. (61) in the form

$$j_x(\chi)=\left(I+\frac{1}{2}\right)\times\left(1-\frac{1}{\chi}\frac{1}{2\Delta}\left(\frac{dE}{dI}\right)^{\text{exp}}\right) \qquad (67)$$

and solve it for χ. The values of the moment of inertia for ^{232}Th and ^{236,238}U obtained in this way are shown in Fig. 31 together with the moment of inertia of the ground-state band for each of these nuclei. The difference between the moments of inertia found in this way and the moments of inertia of the ground-state band can be understood as the result of renormalization due to the polarization effects associated with excitation of the K^- states. This approach evidently increases the renormalization of the moments of inertia, which, as follows from the figure, is small. The figure is also interesting from one further point of view; namely, the moment of inertia J_λ shown in it can be compared with the effective moment of inertia determined by Eqs. (1) and (2) for the 0^- band in the corresponding nuclei.[27,28] The effective moment of inertia decreases with increasing ω^{rot} at the beginning of the 0^- band. We see that this decrease can be described as an effect of the Coriolis mixing of the states in a system whose moment of inertia has normal behavior, i.e., it is an increasing function of the frequency.[75]

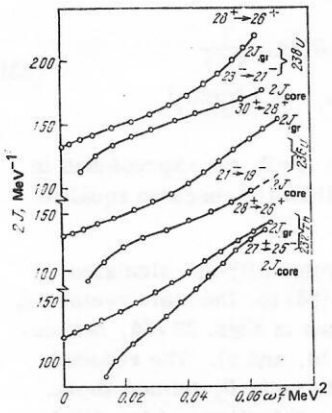

FIG. 31. Moment of inertia of octupole core found from the condition of exact reproduction of the experimental results by the theoretical $j_x(\chi)$ curve. The moments of inertia in the yrast configurations are given for comparison.

Electric characteristics of aligned states.

The simple model of octupole states coupled by Coriolis forces as described earlier is convenient for studying the effects of alignment of the angular momentum on the electromagnetic characteristics of nuclei. As follows from analysis of the available experimental data on the energies of the low-lying negative-parity states in the actinides (see above), such a model is capable of describing qualitatively the spectrum of the 0^- band strongly distorted by the coupling between the vibrations and the rotation. One could therefore expect the conclusions obtained on the basis of this model to have genuine predictive power for electromagnetic transitions as well.

Theoretically, the influence of alignment on the electromagnetic properties of nuclei can be most readily described by considering the example of octupole γ transitions from single-phonon states to states of the ground band. Writing down the expression for the intrinsic part of the operator of the electric octupole moment [see (4)],

$$\mathring{\mathcal{M}}'(E3,\ \tau) = m_0 (b_\tau^+ - (-1)^\tau b_{-\tau}) + \text{Terms that do not contribute to oct} \to \text{gr transitions,} \tag{68}$$

and using the approximate expression (8) for the matrix elements, which holds when $I \gg 1$, we obtain

$$B(E3,\ \text{oct}\ I \to \text{gr}\ I') = |\langle I'_{\text{gr}} | \mathring{\mathcal{M}}'(3,\ I'-I) | I\ \text{oct}\rangle|^2 = m_0^2 (\psi_{\tau=I-I'})^2. \tag{69}$$

In (69), ψ_τ is the weight or the component of the state with projection of the vibrational angular momentum onto the rotation axis equal to τ [see Eqs. (53) and (54)]. The increase in the weight of the $\tau = 3$ component in the states of the 0^- band with increasing angular momentum (see Fig. 25) has the consequence that the dominant octupole $0^- I \to \text{gr} I'$ transitions for $I \gg 1$ are the ones for which $I - I' = 3$, i.e., they are the "directed" octupole transitions, which decrease maximally both the energy and the angular momentum of the nucleus. In the limit of large angular momenta, τ is a state quantum number:

$$\psi_\tau \to \delta_{\tau, j}\ (-3 \leqslant j \leqslant 3), \tag{70}$$

and for octupole transitions from the band j to the ground state there arises the simple selection rule

$$B(E3;\ jI \to \text{gr}\ I') = m_0^2 \delta_{j,\ I-I'}, \tag{71}$$

so that the aligned angular momentum is in this limit a measure of the angular momentum carried from the given state by the octupole γ photon.

It is well known that the probability of an octupole transition with an energy of the order or less than 1 MeV is extremely small. Therefore, such transitions are hardly ever observed experimentally. In reality, octupole states with very large angular momenta are de-excited by collective quadrupole γ photons to states with lower angular momenta without a change in the type of the intrinsic excitation, these states, in their turn, going over to states of the ground band with the emission of dipole γ photons. The structure of the octupole state influences the "branching ratio" of the dipole transitions, i.e., the relative probability of oct $I \to \text{gr} I'$ transitions with different values of I'. The theoretical description of such transitions requires further development of the model, since the operators b_μ^+ and $b_{-\mu}$ of the octupole phonons and the dipole-moment operators $\hat{\mathcal{M}}(1\mu)$ have different transformation properties with respect to the rotation group. Therefore, representation of the dipole operator by a formula like (68) is impossible.

To describe the dipole transitions, we introduce "ideal" dipole operators d_μ^+, d_μ ($\mu = 0, \pm 1$), which we shall assume are vector boson operators. By definition, we shall assume that the dipole phonons d_μ^+ represent degrees of freedom of the nucleus different from the degrees of freedom of the octupole vibrations, so that the operators d_μ^+ and d_μ commute with the operators b_μ^+ and b_μ of the octupole phonons. We represent the electric dipole moment in the form

$$\mathring{\mathcal{M}}(E1,\ \mu) = m_d (d_\mu^+ - (-1)^\mu d_{-\mu}) + \text{Terms unimportant for present consideration.} \tag{72}$$

We shall regard the dipole transitions from the octupole states as the result of coupling between the octupole and dipole degrees of freedom, and we represent the interaction Hamiltonian in the form

$$\mathscr{H}_{d,0} = \sum_{\lambda=2;\ 4} h_\lambda \sum_{\mu\mu'\mu''} (-1)^{\mu+\mu''} C^{\lambda\mu''}_{1\mu'3\mu} \times (d_{\mu'}^+ b_{-\mu} + b_\mu^+ d_{-\mu'}\ (-1)^{\mu-\mu'}) \hat{Q}_{\lambda\mu''}. \tag{73}$$

The operator $\mathscr{H}_{d,0}$ is written down in the laboratory coordinate system to emphasize its scalar nature. The multipole-moment operator $\hat{Q}_{\lambda\mu}$ acts in the space of variables of the core; in what follows, we shall need to know only the expectation values

$$q_{\lambda\tau} = \langle \text{core} | \hat{Q}'_{\lambda\tau} | \text{core} \rangle. \tag{74}$$

The expression (73) is the most general form of operator leading in the first order in the coupling constants h_λ to mixing of the single-phonon states of dipole and octupole type. Thus, there are two coupling constants, h_2 and h_4, and in what follows we shall consider the two limiting cases when one of them plays a dominant role. We shall refer to these two cases as the variants with quadrupole and hexadecapole coupling of excitations of dipole and octupole type.

The intrinsic part of the Hamiltonian of the nucleus in the K representation now has the form

$$\mathcal{H}_{\text{intr}}=\sum_K \omega_{|K|} b_K^+ b_K+\sum_{K'} \omega^d_{|K'|} d^+_{K'} d_{K'}+\mathcal{H}_{d,0}. \quad (75)$$

Assuming that the interaction $\mathcal{H}_{d,0}$ is weak [as a rule, the B(E1) factors of the transitions from the octupole states are small fractions of the single-particle unit], the coupling (73) can be taken into account in the first order in h_λ by introducing the renormalized phonon operators

$$\sigma^+_\mu=b^+_\mu+\sum_{\lambda=2,4}\frac{h_\lambda}{\Delta\omega}\sqrt{\frac{2\lambda+1}{7}}\sum_{\mu'} C^{3\mu}_{1\mu',\lambda\mu-\mu'} Q_{\lambda\mu-\mu'} d^+_{\mu'}. \quad (76)$$

In (76), $\Delta\omega=\omega^d_K-\omega^{\text{oct}}_K$, and it is assumed that $\Delta\omega$ does not depend on K or K'.

Using again the high-spin approximation for the matrix elements described in Sec. 1, we find

$$\langle I_2\,\text{gr}\,|\hat{\mathcal{M}}(E1,\ \tau=I_2-I_1)|I_1\,\text{oct}\rangle$$
$$=(-1)^{\tau+1} m_d \sum_{\lambda=2,4}\sqrt{\frac{2\lambda+1}{7}}\frac{h_\lambda}{\Delta\omega}\sum_{\tau'} C^{3\tau'}_{1,-\tau;\lambda\tau+\tau',\lambda\tau+\tau'} q_{\lambda\tau+\tau'}\psi_{\tau'}, \quad (77)$$

where $\psi_{\tau'}$ are again the weights of the components with different projections of the vibrational angular momentum onto the rotation axis.

The expectation values (moments) $q_{\lambda\tau}$ [Eq. (74)] may depend on the angular momentum of the state. If the intrinsic coordinate system is chosen in such a way that the inertia tensor in it has diagonal form, then

$$q_{2K}=q_2\left(\cos\gamma\delta_{K0}+\frac{\sin\gamma}{\sqrt{2}}(\delta_{K,2}+\delta_{K,-2})\right). \quad (78)$$

As the calculations show, the branching ratios of the transitions depend weakly on the nonaxiality angle γ. Therefore, to study the branching ratios of transitions from states with spins of order $(10-20)\hbar$ it is sufficient to consider the axial case $\gamma=0$.

For an axial nucleus, we also have

$$q_{4K}=q_4\delta_{K,0}. \quad (79)$$

We consider separately the parametrization (79), and also the variant in which the hexadecapole coupling of the dipole and octupole degrees of freedom arises as a result of rotation. If the Coriolis forces are important in the formation of the multipole moments (74), one can hope to take them into account by setting

$$q_{4K}=q'_4(\delta_{K,1}-\delta_{K,-1}). \quad (80)$$

In the general case, a different parametrization of the moments q_{4K} is also obviously possible.

The expressions for the B(E1) factors of transitions from the octupole states of negative signature for the variants (78), (79), and (80) have the following form:

a) $\lambda=2$,

$$B(E1;\ \text{oct}\,I\to\text{gr}\,I\mp1)=B_2\frac{1}{3}\left\{\frac{\sqrt{15}}{2}\psi_{\pm3}-\psi_{\pm1}+\frac{1}{2}\psi_{\mp1}\right\}, \quad (81)$$
$$B_2=\frac{9}{14}\left(\frac{m_d h_2 q_2}{\Delta\omega}\right)^2;$$

b) $\lambda=4$, $K=0$,

$$B(E1;\ \text{oct}\,I\to\text{gr}\,I\mp1)=B_4\left\{\frac{1}{16}[\psi_{\mp3}7\sqrt{5}-\psi_{\mp1}5\sqrt{3}+\psi_{\pm1}3\sqrt{3}-\psi_{\pm3}\sqrt{5}]\right\}, \quad (82)$$
$$B_4=\frac{81}{14}\left(\frac{m_d h_4 q_4}{\Delta\omega}\right)^2;$$

c) $\lambda=4$, $|K|=1$,

$$B(E1;\ \text{oct}\,I\to\text{gr}\,I\mp1)=B'_4\left\{\psi_{\pm3}\frac{1}{4\sqrt{5}}-\psi_{\mp1}\frac{\sqrt{3}}{4}+\psi_{\mp3}\frac{7}{2\sqrt{5}}\right\},\quad B'_4=\frac{5}{14}\left(\frac{h_4 q'_4 m_d}{\Delta\omega}\right)^2. \quad (83)$$

In the absence of alignment, $\chi=0$, the expressions in the curly brackets in Eqs. (81)–(83) become equal to unity for B(E1; $0^-\to$ gr).

The reduced transition probabilities, calculated in accordance with Eqs. (81)–(83) for the state vectors ψ_τ determined above, are shown in Figs. 32–34, respectively, for the variants a), b), and c). The reduced probabilities are given in the units B_λ defined above. The figures show clearly the selectivity of the dipole transitions with respect to the angular momentum of the final state. This selectivity is manifested particularly clearly in the transitions from the 0^- band distorted by the action of the Coriolis forces. In contrast to what we had for the octupole transitions, the selectivity of the dipole transitions depends on the type of coupling between the dipole and octupole degrees of freedom.

The rather complicated relationships between the probabilities of the different dipole transitions for $I\gg1$ that follow from our theoretical treatment have a very simple geometrical interpretation. In the lowest octupole-excited state with large angular momentum, the vibrational angular momentum is directed parallel to the angular momentum of the rotation of the core (see the left-hand part of Fig. 35). To obtain such a state in the first order of perturbation theory as a result of the influence of the electric dipole moment (the central part of Fig. 35) on the wave function of the ground-state band of the core (the right-hand part of Fig. 35), it is necessary to take into account the quantum-mechanical rules for adding angular momenta. For $I\gg1$, these rules simplify, and the "kinematically" most probable transitions correspond to the classical rules of addition. Since the dipole operator which participates in the transition has a complicated structure and acts on the core of the nucleus and on the phonon part of the wave function, the rules of addition affect the vibrational and rotational functions and for aligned states lead to the selection rule $0^-I\to\text{gr}\,I-3+\lambda$,

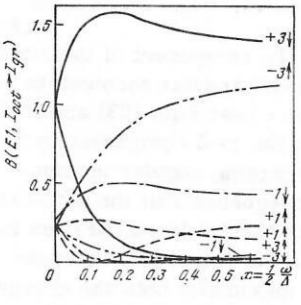

FIG. 32. Reduced probabilities B(E1, $j_x I\to\text{gr}\,I'$) for transitions from j_x octupole bands of negative signature to the ground-state band for the variant $\lambda=2$. On the right, we give the asymptotic values of the aligned angular momentum j_x in the corresponding band and the type of transition: ↓) $I'=I-1$; ↑) $I'=I+1$. The normalization of the B(E1) factors corresponds to $B=1$ at $\chi=0$.

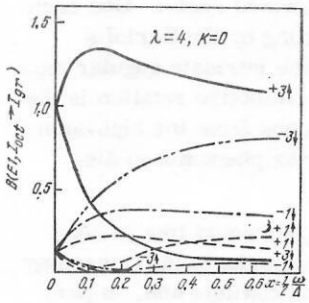

FIG. 33. The same as in Fig. 31 for the variant of the theory with $\lambda = 4$, $K = 0$.

where λ is a characteristic of the type of the coupling of the dipole and octupole degrees of freedom. For $\lambda = 2$, the de-excitation of an octupole excitation of an aligned band is associated with a decrease in the angular momentum of the state, whereas for $\lambda = 4$ the emission of a dipole phonon from a state of an aligned band leads to an increase in the angular momentum of the system.

Arguments similar to those given above in connection with Fig. 35 can be used to analyze dipole transitions from other octupole bands. The tendencies for transitions from the "antialigned" band $j = -3$ to the ground-state band have an obvious geometrical interpretation. We note that the classical rules for adding angular momenta do not permit the formation of $|j| \neq 3$ states from an yrast-band state of the nucleus (without excitation of nutation-type motion). Therefore, the $B(E1)$ factors for transitions from the $j = \pm 3$ bands are distinguished by their magnitude among all the remaining dipole transitions.

Turning to a comparison of the theoretical conclusions with the experimental data, we note that the deviations in the branching ratios of the E1 transitions from Alaga's rules[7] in nuclei whose spectra are distorted by the effect of the Coriolis forces have long been noted in the literature.[66] It can be assumed that the coupling between the octupole and dipole degrees of freedom in nuclei is largely determined by the static deformation of the average field of the nucleus.[82] Because of the distinguished part played by the quadrupole static deformation relative to deformations of higher multipolarity, it is to be expected that the effects of the

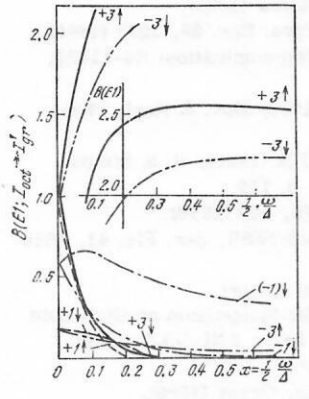

FIG. 34. The same as in Fig. 31 for the variant of the theory with $\lambda = 4$, $|K| = 1$.

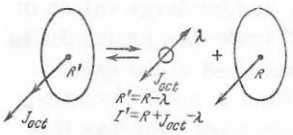

FIG. 35. Geometrical interpretation of selection rules for dipole transitions from octupole bands

quadrupole coupling will also be predominant in the transition probabilities. However, there are no grounds for eliminating the possibility of hexadecapole coupling, particularly in the cases when the Coriolis forces distort the core, since the importance of the Coriolis forces increases with increasing intrinsic angular momentum associated with the intrinsic excitation.

As follows from the above analysis of the spectra of the 0^- band in the actinides, alignment of the vibrational angular momentum is already noticeable in states with angular momentum $I = 5$ [for ^{238}U, the value of χ as determined from the data given in Fig. 27 for $\tilde{I} = (I_1 + I_2)/2 = 6$ is $\chi = 0.093$; at the same time, $j_x = 1.74$ and $\psi_{\tau=3} = 0.81$]. Judging from Figs. 32–34, the selectivity of the dipole transitions with respect to the angular momentum of the final state must already be clearly expressed at such values of χ. This conclusion agrees with the existing experimental data. As a rule, $I \to I \pm 1$ dipole transitions from states of the 0^- band can be measured simultaneously only for $I \leq (5-7)\hbar$. At higher spins, only half the kinematically possible transitions are detected.

An example of the emission spectrum of a Coulomb-excited nucleus is given in Fig. 1 in Ref. 66. In this example, which is for the nucleus ^{238}U, one can clearly trace the $0^- I \to \mathrm{gr}\, I - 1$ transitions for states of the octupole band up to $I \leq 17\hbar$. The last experimentally resolved transition of the $0^- I \to \mathrm{gr}\, I + 1$ type corresponds to $I = 3$. There may also be detection of the $5^- \to 6^+$ and $7^- \to 8^+$ transitions, whose energy is equal to the energy of the other transitions. In any case, the probability of the $5^- \to 6^+$ and $7^- \to 8^+$ transitions is appreciably less than the $5^- \to 4^+$ and $7^- \to 6^+$ probability. We note that for the variant with quadrupole coupling $B(E1; 7^- \to 8^+)/B(E1; 7^- \to 6^+) \approx 0.2$, this ratio decreasing rapidly with increasing angular momentum. Thus, the analyzed example of the spectrum can be explained qualitatively by the presence of quadrupole coupling of the octupole and dipole degrees of freedom. Unfortunately, a quantitative analysis of the expreimental data is impossible, owing to the absence of data on the intensity of the γ radiation.

The example analyzed above can be described as typical, and a similar enhancement of the $I^- \to (I-1)^+$ transitions is noted in the nuclei of the rare-earth elements. However, a different situation has also been found experimentally. Figure 5 (Ref. 27) shows the spectrum of the γ radiation of ^{232}Th. The radiation spectrum in this nucleus corresponds most closely to the variant $K = 4, \lambda = 1$, in which alignment leads to a rapid increase in the relative probability of the $I^- \to (I+1)^+$ transitions. This variant of the theory gives the value $B(E1; 5^- \to 6^+)/B(E1; 5^- \to 4^+) \approx 20$, which is

close to the experimental value, and for large values of I leads to such small $I^- \to (I-1)^+$ transition probabilities that their detection under the conditions of the experiment in Ref. 27 is impossible. Indeed, such transitions in the spectrum in Fig. 5 cannot be seen, whereas the $I^- \to (I+1)^+$ lines can be traced up to $I = 13$.

Thus, the conclusions of the theory with regard to the influence of alignment on the electric properties of nuclei also find a certain experimental confirmation. The interpretation of the results of calculation of the $B(E1)$ factors in accordance with the formulas of the phenomenological model that we have given by means of Fig. 35 makes it possible to formulate general tendencies for the transition probabilities that can be expected under conditions when there is alignment of the angular momentum associated with an individual degree of freedom α of the nucleus. We denote by j_α the aligned angular momentum in the state α. In the transition j_α, $I \to \mathrm{gr}, I'$ the projection of the intrinsic angular momentum onto the rotation axis must change by j_α units. The total angular momentum changes in such a way that $I - I' = j_\alpha + \Delta R$, where ΔR is the change in the collective rotational angular momentum R. The variations in R are bounded by the inequality $|j_\alpha - l| \leq \Delta R \leq j_\alpha + l$, where l is the multipolarity of the transition, and, as we have seen in the example analyzed above, they are due to the interaction between the different degrees of freedom of the nucleus. Therefore, the transition probabilities can contain valuable information about the coupling of the different degrees of freedom.

CONCLUSIONS

The accumulation of experimental information on high-spin states of nuclei has opened up new possibilities for studying their structure. This has made it possible to see how restricted is the adiabatic picture of the structure of deformed nuclei and to obtain estimates of the limits of its applicability. Rotation of nuclei leads to coupling of the rotational bands and is manifested in deviations of the energies of the states and the transition probabilities between them from the predictions of the adiabatic theory. Sometimes the deviations are very pronounced (backbending, branching ratios of the E1 transitions).

Evidently, the most important result of the theoretical analysis of the high-spin states is the possibility of generalizing the methods developed for describing the adiabatic characteristics of nuclei [moments of inertia, $B(\lambda)$ factors, etc.] without significant adjustment to the basic ideas of nuclear structure in order to describe numerous experimental data on high-spin states. The main element in this generalization of the theory is the transition to quasiparticle configurations in a rotating average field. For moderately rapid rotation of the nuclei ($I \lesssim 30\hbar$), the main role is played by mixing of the adiabatic bands by the Coriolis forces, the effects of which have been discussed in detail above.

It is worth noting once more that the effects of the Coriolis interaction are in some cases manifested very clearly and then lead to qualitative changes in the tendencies whose discovery provided the basis of our notions about the structure of deformed nuclei. One such clear manifestation of the coupling by the Coriolis forces leading to alignment of the intrinsic angular momentum in the direction of the collective rotation is the selectivity in the dipole transitions from the high-spin negative-parity states; this is the phenomenon discussed in Sec. 3.

One of the authors (C. Briançon) would like to take this opportunity to express this thanks to the Governing Board and members of the Joint Institute and, in particular, Professor V. G. Solov'ev for hospitality at the Laboratory of Theoretical Physics, where the present work was done.

[1]K. Alder *et al.*, Rev. Mod. Phys. **28**, 432 (1956).
[2]A. Bohr, K. Dan. Vidensk. Selsk. Mat.-Fys. Medd. **26**, No. 14 (1952); A. Bohr and B. R. Mottelson, K. Dan. Vidensk. Selsk. Mat.-Fys. Medd. **27**, No. 16 (1953).
[3]K. Alder and A. Winther, Coulomb Excitation, Academic Press (1966).
[4]K. Alder and A. Winther, Electromagnetic Excitation, N. M., Amsterdam (1975).
[5]C. Briançon, Proc. Summer School, Predeal (1978).
[6]D. Schwalm, GSI Preprint, 80-26 (1980).
[7]G. Alaga *et al.*, K. Dan. Vidensk. Selsk. Mat.-Fys. Medd. **29**, No. 9 (1955).
[8]A. K. Kerman, K. Dan. Vidensk. Selsk. Mat.-Fys. Medd. **30**, No. 15 (1956).
[9]J. de Bettancourt *et al.*, Izv. Akad. Nauk SSSR, Ser. Fiz. **40**, 2041 (1976); Rapport d' Activité CSNSM (Orsay) (1976–1977), p. 28.
[10]B. R. Mottelson and J. P. Valatin, Phys. Rev. Lett. **5**, 511 (1960).
[11]Yu. T. Grin', Zh. Eksp. Teor. Fiz. **41**, 445 (1961) [Sov. Phys. JETP **14**, 320 (1962)].
[12]A. Johnson, M. Ryde, and J. Sztarkier, Phys. Rev. B **34**, 605 (1971).
[13]D. L. Hillis *et al.*, Nucl. Phys. **A325**, 216 (1979).
[14]F. S. Stephens, Rev. Mod. Phys. **47**, 43 (1975).
[15]I. N. Mikhaĭlov, K. Neergard, *et al.*, Fiz. Elem. Chastits At. Yadra **8**, 1338 (1977) [Sov. J. Part. Nucl. **8**, 550 (1977)].
[16]I. N. Mikhaĭlov, Soobshchenie (Communication) R4-7862, JINR, Dubna (1974).
[17]A. Bohr and B. R. Mottelson, Nuclear Structure, Vol. 2, Benjamin, New York (1969) [Russian translation published by Mir, Moscow (1977)].
[18]F. G. Filippov, Fiz. Elem. Chastits At. Yadra **4**, 992 (1974) [Sov. J. Part. Nucl. **4**, 405 (1974)].
[19]D. A. Varshalovich, L. N. Moskalev, and V. K. Khersonskiĭ, Kvantovaya teoriya uglovogo momenta (Quantum Theory of Angular Momentum), Mir, Moscow (1975).
[20]T. Holstein and M. Primakoff, Phys. Rev. **58**, 1098 (1940).
[21]I. N. Mikhaĭlov, Soobshchenie (Communication) R4-11424, JINR, Dubna (1978).
[22]D. Yanssen, Yad. Fiz. **25**, 897 (1977) [Sov. J. Nucl. Phys. **25**, 479 (1977)].
[23]R. Simon *et al.*, Z. Phys. **A298**, 121 (1980); R. S. Simon *et al.*, GSI Annual Report (1978), p. 164.
[24]P. O. Tjøm *et al.*, Phys. Lett. **B72**, 439 (1978).
[25]C. Briançon *et al.*, Izv. Akad. Nauk SSSR, Ser. Fiz. **41**, 1986 (1977).
[26]C. Briançon *et al.*, CSNSM Annual Report.
[27]C. Briançon *et al.*, in: Proc. of the Symposium on High-Spin Phenomena in Nuclei, Argonne, 1979, ANL/PLY-79-4; Orsay Annual Report (1976–1978).
[28]A. Lefebvre, Thèse de 3-m Cycle, Orsay (1980).
[29]R. S. Simon *et al.*, Z. Phys. **A298**, 121 (1980).
[30]C. Brainçon *et al.*, in: Proc. of the Intern. Conf. on Nuclear

Structure in Heavy-Ion Reactions, Bucharest (1981).
[31]E. Grosse *et al.*, GSI Preprint 81-5; Proc. of the Nobel Symposium on Nuclei at Very High Spins (1980) (to be published in Phys. Scr.).
[32]R. S. Simon *et al.*, GSI and CSNSM Annual Report (1978–1980).
[33]A. Lefebvre *et al.*, Verhandlungen der Deutschen Physikalischen Gesselschaft Physikal, Hamburg (1981)—Kern-bundteichen Physik, p. 804.
[34]R. Kulessa *et al.*, GSI Annual Report (1980); GSNSM (Orsay) Annual Report (1978–1980).
[35]P. Fuchs *et al.*, GSI Annual Report (1977), GSI-J-I-78, p. 195.
[36]E. Grosse, in: Symposium on High-Spin Phenomena in Nuclei, ANL-PHY-79-4, Argonne (1979).
[37]M. Ower *et al.*, in: Proc. of the Intern. Conf. on Nuclear Behavior at High Angular Momenta, Strasbourg (1980); J. Phys. C **10**, 119 (1980).
[38]R. S. Piercey, Phys. Rev. Lett. **46**, 415 (1981).
[39]L. Münchow and H. Schulz, Fiz. Elem. Chastits At. Yadra **12**, 1001 (1981) [Sov. J. Part. Nucl. **12**, 403 (1981)].
[40]A. Bohr and B. R. Mottelson, in: Intern. Conf. on Nuclear Structure, Tokyo (1977); J. Phys. Soc. Jpn. Suppl. **44**, 157 (1978).
[41]R. Bengtsson and S. Frauendorf, Nucl. Phys. **A327**, 139 (1979).
[42]L. L. Riedinger, Nucl. Phys. A347, 141 (1980).
[43]R. M. Lieder, Nucl. Phys. **A347**, 69 (1980).
[44]L. L. Riedinger *et al.*, Phys. Rev. Lett. **44**, 568 (1980).
[45]R. Bengtsson, in: Proc. of the Intern. Conf. on Nuclear Behavior at High Spins, Strasbourg (1980).
[46]Yu. T. Grin', Fiz. Elem. Chastits At. Yadra **6**, 1105 (1975) [Sov. J. Part. Nucl. **6**, 446 (1975)].
[47]T. Byrski *et al.*, in: Intern. Conf. on Nuclear Behavior at High Angular Momenta, Strasbourg (1980); Contributions, p. 87.
[48]L. Funke *et al.*, Nucl. Phys. **A355**, 228 (1981).
[49]J. D. Garret *et al.*, Phys. Rev. Lett. **47**, 75 (1981).
[50]F. S. Stephens and R. S. Simon, Nucl. Phys. **A138**, 257 (1972).
[51]A. Faessler, in: Intern. Conf. on Nuclear Behavior at High Spins; J. Phys. C **10**, 143 (1980).
[52]R. Bengtsson and S. Frauendorf, Nucl. Phys. **A314**, 27 (1979).
[53]R. Bengtsson, I. Hamamoto, and B. R. Mottelson, Phys. Lett. **B73**, 259 (1978).
[54]P. Ring, H. J. Mang, and B. Banerjee, Nucl. Phys. **A225**, 141 (1974).
[55]A. Faessler *et al.*, Nucl. Phys. **A256**, 106 (1976).
[56]A. Faessler, K. R. Sandhya Devi, and A. Barroso, Nucl. Phys. **A286**, 101 (1977).
[57]A. Faessler, M. Ploszajczak, and K. R. Sandhya Devi, Nucl. Phys. **A301**, 529 (1978).
[58]A. L. Goodman, Nucl. Phys. **A256**, 113 (1976).
[59]S. Frauendorf and R. S. Simon, GSI Preprint 80-25.
[60]V. G. Soloviev and P. Vogel, Phys. Lett. **6**, 126 (1963).
[61]V. G. Solov'ev, P. Fogel', and A. A. Korneĭchuk, Izv. Akad. Nauk SSSR, Ser. Fiz. **28**, 1599 (1964).
[62]A. Faessler and A. Plastino, Z. Phys. **203**, 333 (1967).
[63]J. Kochbach and P. Vogel, Phys. Lett. **B32**, 434 (1970).
[64]K. Neergard and P. Vogel, Nucl. Phys. **A145**, 33 (1970); **A149**, 209, 217 (1970).
[65]P. Vogel, Phys. Lett. **B60**, 431 (1976).
[66]E. Grosse *et al.*, Phys. Lett. **35**, 565 (1975).
[67]P. Fuchs *et al.*, Annual Report (1978), p. 195.
[68]M. Fenzl *et al.*, Z. Phys. **A273**, 163 (1975).
[69]P. M. Walker *et al.*, Phys. Lett. **B87**, 339 (1979).
[70]G. D. Dracoulis, in: Proc. of the Intern. Conf. on Nuclear Behavior at High Spins, Strasbourg (1980).
[71]D. R. Zolnowski *et al.*, Phys. Lett. **B55**, 453 (1975).
[72]M. Ploszajczak and A. Faessler, Z. Phys. **A283**, 349 (1977).
[73]F. W. N. de Boer *et al.*, Z. Phys. **A284**, 267 (1978).
[74]J. Konijn *et al.*, Z. Phys. **A284**, 233 (1978).
[75]R. B. Begzhanov *et al.*, Izv. Akad. Nauk SSSR, Ser. Fiz. **43**, 1027 (1979).
[76]I. N. Mikhaĭlov, in: Lektsii Mezhdunarodnoĭ letneĭ shkoly po strukture yadra (Lectures at the Intern. Summer School on Nuclear Structure), Alushta, 1980, D4-80-385, JINR.
[77]F. W. De Boer *et al.*, in: Proc. of the Symposium on High-Spin Phenomena in Nuclei, ANL/PHY-97-4, Argonne (1979).
[78]R. K. Sheline *et al.*, Phys. Rev. Lett. **41**, 374 (1978).
[79]M. Abramowitz and I. A. Stegun (Eds.), Handbook of Mathematical Functions, Dover, New York (1965) [Russian translation published by Nauka, Moscow (1979), p. 27].
[80]L. D. Landau and E. M. Lifshits, Kvantovaya mekhanika, Nauka, Moscow (1977); English translation: Quantum Mechanics, Pergamon, Oxford (1974).
[81]S. P. Ivanova, A. L. Komov, L. A. Malov, and V. G. Solov'ev, Izv. Akad. Nauk SSSR Ser. Fiz. **39**, 1286 (1975).
[82]M. I. Baznat, N. I. Pyatov, and D. I. Salamov, Yad. Fiz. **25**, 1155 (1977) [Sov. J. Nucl. Phys. **25**, 613 (1977)].

Translated by Julian B. Barbour